

CHALMERS



Pulse Pressure Variation Estimation to Predict Fluid Responsiveness

Master of Science Thesis

Nassim Tayari

*Department of Signal and Systems
Division of Biomedical Engineering
Chalmers University of Technology
Gothenburg, Sweden. 2010.
Report No: EX090/2010*

Acknowledgements

First of all, I like to thank my family, my father, mother and brother for their love, listening and supporting all over my life and especially last couple of years.

I deeply thank my supervisors both at Chalmers University of technology and Sahlgrenska University hospital.

I would like to record my gratitude to Professor Tomas Mckelvey at the department of signals and systems at Chalmers University of Technology for his supervision, advice, and guidance from the very early stage of this research.

I am heartily thankful to Dr.Soren Sondergaard, head of department of Anaesthesia - General Surgery- at Sahlgrenska University Hospital whose encouragement, guidance and support from the initial to the final level enabled me to develop an understanding of the subject.

Lastly, I offer my regards and blessings to my friends and all of those who supported me in any respect during the completion of the project.

Nassim Tayari

Gothenburg.December2010.

Abstract

Numerous studies have shown the pulse pressure variation in arterial blood pressure due to respiratory cycle as one of the most accurate predictors of fluid responsiveness in mechanically ventilated patients. In the operating room fluid administration based on pulse pressure variation monitoring helps the physician in decision making - whether to volume resuscitate or use interventions - in patients undergoing high risk surgery.

In cooperation with the anaesthetic department, surgical suites North at Sahlgrenska University Hospital, Gothenburg, pulse pressure variation was estimated by implementing an improved automatic algorithm introduced by M.Aboy et al. The method is based on automatic beat detection algorithm for beat segmentation, kernel smoother for envelope estimation and rank order filters. The implemented algorithm results were validated comparing against a commercial system (LiDCO™) and showing that the implemented algorithm provides continuous measurement of the pulse pressure variation during abrupt hemodynamic changes. The algorithm was put into clinical use in selected patients to investigate the effect of volume expansion as well as intrathoracic pressure on pulse pressure variation. Additionally the relationship between variations in Positive End Expiratory Pressure was examined based on an animal study.

Keywords: Pulse Pressure Variation, Fluid Responsiveness. Cardiovascular signals, Pressure signals

Contents

Acknowledgements.....	2
Abstract.....	3
Table of Figures	6
Table of Tables	8
Notations and Abbreviations.....	9
Chapter 1: Introduction.....	11
Chapter 2 : Physiological Background	13
<i>The Heart, a pump within a pump – two circulatory systems intertwined with the airways</i>	13
<i>The Frank Starling Curve or cardiac function curve.....</i>	14
<i>Venous Return</i>	15
<i>The Cardiac Cycle.....</i>	18
Chapter 3 : Pulse Pressure Variation Estimation	21
3.1 Introduction	21
3.1.1 Pulse Pressure variation	21
3.1.2 Pressure Pulse Morphology	22
3.2 Algorithm Description.....	22
3.2.1 Step 1: Beat Detection and Segmentation.....	23
3.2.2 Step 2: Beat Maxima Detection	33
3.2.3 Step 3: Envelope Estimation.....	33
3.2.4 Step 4: PPV Estimation.....	35
3.3 Methods: Algorithm Assessment	36
3.3.1 Beat Detection.....	36
3.3.2 PPV Estimation.....	37

Chapter 4 : Evaluation of the influence of tidal insufflations pressure on the capacity of pulse pressure variation (PPV) to predict fluid responsiveness.	39
4.1 Introduction	39
4.2 Methodology	40
4.2.1 Patient Study	40
4.2.2 Animal Study	40
4.3 Results	41
4.3.1 Patient Study Results:	41
4.3.2 Animal Study Results	53
Chapter 5 : Discussion and Conclusion	61
References	64

Table of Figures

FIGURE 1 CARDIAC FUNCTION CURVE .	14
FIGURE 2 SIMULTANEOUS PLOTS OF THE CARDIAC AND VASCULAR FUNCTION CURVES	15
FIGURE 3 SIMULTANEOUS PLOTS OF THE CARDIAC AND VASCULAR FUNCTION CURVES OR VENOUS RETURN CURVE..	17
FIGURE 4 SIMULTANEOUS PLOTS OF THE CARDIAC AND VASCULAR FUNCTION CURVES OR VENOUS RETURN CURVE..	17
FIGURE 5.SIMULTANEOUS PLOTS OF THE CARDIAC AND VASCULAR FUNCTION CURVES OR VENOUS RETURN CURVE..	18
FIGURE 6 ARTERIAL BLOOD PRESSURE IN RELATION TO THE PRESSURE AND THE VOLUME IN THE LEFT VENTRICLE..	19
FIGURE 7 ARTERIAL BLOOD PRESSURE WAVEFORM COMPONENTS.	22
FIGURE 8 BLOCK DIAGRAM OF COMMON STRUCTURE OF DETECTION ALGORITHMS.....	23
FIGURE 9 BLOCK DIAGRAM OF THE ARCHITECTURE OF DETECTION ALGORITHM	24
FIGURE 10 WAVEFORM COMPONENTS –MAXIMA AND MINIMA- ON AN ABP SIGNAL..	25
FIGURE 11 THE RAW BLOOD PRESSURE SIGNAL (BLUE CURVE) AND HP FILTERED SIGNAL IN BLACK CURVE AS WELL AS BAND PASSED FILTERED SIGNAL	27
FIGURE 12 RANK ORDER FILTER CLASSIFICATION RESULTS ON THE RAW SIGNAL .	29
FIGURE 13 RANK ORDER FILTER CLASSIFICATION RESULTS ON THE FILTERED SIGNAL.....	30
FIGURE 14 RANK ORDER FILTER CLASSIFICATION RESULTS ON THE RAW SIGNAL.	30
FIGURE 15 FILTERED SIGNAL RANK ORDER FILTER CLASSIFICATION RESULTS .	31
FIGURE 16 AUTOMATIC BEAT DETECTION . $A_i = (A_1, A_2, \dots, A_N)$ ARE SAMPLE INDICES CORRESPONDING TO THE BEGINNING OF EACH BEAT AND $B_i = (B_1, B_2, \dots, B_N)$ ARE SAMPLE INDICES RELATIVE TO THE MAXIMA OF EACH BEAT.	32
FIGURE 17 STEP 1. AUTOMATIC BEAT DETECTION AND PULSE PRESSURE CALCULATION	33
FIGURE 18 UPPER AND LOWER ENVELOPE ESTIMATIONS ARE PRESENTED BY $U(N)$ AND $L(N)$ RESPECTIVELY.	35
FIGURE 19 RELATIONSHIP BETWEEN PPV_{LIDCo} AND PPV_{AUTO}	38
FIGURE 20 BLAND ALTMAN ANALYSIS FOR PPV_{LIDCo} AND PPV_{AUTO}	38
FIGURE 21 PPV IS REPRESENTED IN (A) LIKEWISE PPV MEAN OVER FOUR RESPIRATORY CYCLES FOR MV 6.5 L/MIN.	42
FIGURE 22 PPV AND PPV MEAN OVER FOUR RESPIRATORY CYCLES FOR MV 7.5 L/MIN	42
FIGURE 23 PPV AND PPV MEAN OVER FOUR RESPIRATORY CYCLES FOR MV 5.5 L/MIN.....	43
FIGURE 24 PPV AND PPV MEAN OVER FOUR RESPIRATORY CYCLES AFTER 1ST VOLUME EXPANSION	44
FIGURE 25 PPV AND PPV MEAN OVER FOUR RESPIRATORY CYCLES 2ND FIRST VOLUME EXPANSION.	44
FIGURE 26 PPV AND PPV MEAN OVER FOUR RESPIRATORY CYCLES AFTER THIRD VOLUME EXPANSION.....	45
FIGURE 27 PPV AND PPV MEAN OVER FOUR RESPIRATORY CYCLES .	45
FIGURE 28 PPV AND PPV MEAN OVER FOUR RESPIRATORY CYCLES AFTER 4TH VOLUME EXPANSION	46
FIGURE 29 PRE-ANAESTHETIC STAGE : PPV AND PPV MEAN OVER FOUR RESPIRATORY CYCLES	48
FIGURE 30 FLUID CHALLENGE: MV 5.8 L/MIN .PPV AND PPV MEAN OVER FOUR RESPIRATORY CYCLES	49

FIGURE 31 FLUID CHALLENGE: MV 6.6 L/MIN .PPV AND PPV MEAN OVER FOUR RESPIRATORY CYCLES ARE REPRESENTED IN A AND B RESPECTIVELY.....	49
FIGURE 32 FLUID CHALLENGE: MV 7.4 L/MIN .PPV AND PPV MEAN OVER FOUR RESPIRATORY CYCLES	50
FIGURE 33 PRE-INFUSION OF COLLOID PPV AND PPV MEAN OVER FOUR RESPIRATORY CYCLES	50
FIGURE 34 VASOPRESSOR CHALLENGE: PER INFUSION .PPV AND PPV MEAN OVER FOUR RESPIRATORY CYCLES	51
FIGURE 35 POST INFUSION STAGE : PPV AND PPV MEAN OVER FOUR RESPIRATORY CYCLES	51
FIGURE 36 POST OPERATION STAGE : PPV AND PPV MEAN OVER FOUR RESPIRATORY CYCLES	52
FIGURE 37 VENTILATION IN NORMAL VENTILATOR MODE AT PEEP 5 CM H ₂ O	54
FIGURE 38 AFTER LAVAGE –THE PROCESS OF WASHING LUNGS WITH SALINE-VENTILATION IN NORMAL VENTILATOR MODE.....	54
FIGURE 39 AFTER RECRUITMENT MANOEUVRE , VENTILATION IN HFJV MODE AT PEEP 20 CM H ₂ O.	55
FIGURE 40 AFTER RECRUITMENT MANOEUVRE , VENTILATION IN HFJV MODE AT PEEP 17 CM H ₂ O.	55
FIGURE 41 AFTER RECRUITMENT MANOEUVRE , VENTILATION IN HFJV MODE AT PEEP 14 CM H ₂ O.	56
FIGURE 42 AFTER RECRUITMENT MANOEUVRE , VENTILATION IN HFJV MODE AT PEEP 14 CM H ₂ O.	56
FIGURE 43 AFTER RECRUITMENT MANOEUVRE, VENTILATION IN HFJV MODE AT PEEP 8 CM H ₂ O.	57
FIGURE 44 AFTER RECRUITMENT MANOEUVRE, VENTILATION IN HFJV MODE AT PEEP 5CM H ₂ O.....	57
FIGURE 45 NORMAL VENTILATION MODE PEEP =5CM H ₂ O AFTER FIRST RECRUITMENT MANOEUVRE.	58
FIGURE 46 AFTER SECOND RECRUITMENT MANOEUVRE, VENTILATION IN NORMAL MODE AT PEEP 14 CM H ₂ O.	58
FIGURE 47 AFTER SECOND RECRUITMENT MANOEUVRE, VENTILATION IN NORMAL MODE AT PEEP 11 CM H ₂ O.	59

Table of Tables

TABLE 1. VALIDATION OF THE ALGORITHM'S PERFORMANCE COMPARED TO THE PROFESSIONAL ANNOTATION OF TWO ABP SIGNALS..	37
TABLE 2 MV CHALLENGE: RELATIONSHIP BETWEEN (PPV) AND (MVV).....	46
TABLE 3 FLUID CHALLENGE: RELATIONSHIP BETWEEN (PPV) AND (VE)	47
TABLE 4 VARIATION IN PPV IN DIFFERENT STAGED DURING SURGERY	52
TABLE 5 THE RELATIONSHIP BETWEEN PPV AND PEEP VARIATION	60

Notations and Abbreviations

Abbreviation	Description
AAMI	Association For The Advancement Of Medical Instrumentation
ABP	Arterial Blood Pressure
ALI	Acute Lung Injury
AP	Aortic Pressure
ARDS	Acute Respiratory Distress Syndrome
BSA	Body Surface Area
CI	Cardiac Index
CO	Cardiac Output
EDV	End Diastolic Volume
ESV	End Systolic Volume
HR	Heart Rate
HFJV	High Frequency Jet Ventilation
IBI	Inter-Beat Interval
LAP	Left Atrial Pressure
LVV	Left Ventricular Volume
LVP	Left Ventricular Pressure
MVV	Minute Volume Variations
OR	Operation Room
PCWP	Pulmonary Capillary Wedge Pressure
PEEP	Positive End-Expiratory Pressure
PMS	Mean Systemic Filling Pressure
PPV	Pulse Pressure Variation
PSD	Power Spectral Density

RAP	Right Atrial Pressure
RVR	Resistance To Venous Return
RV SV	Right Ventricle Stroke Volume
SNR	Signal To Noise Ratio
SV	Stroke Volume
TS	Twin Stream
VE	Volume Expansion

Chapter 1: Introduction

Objective:

Why estimation of pulse pressure variation matters?

The presence of pulse pressure variations (PPV) of a certain dignity is a dynamic indicator of fluid responsiveness under given conditions of controlled ventilation, i.e. there is an option of increasing flow, cardiac output (CO), by fluid resuscitating the patient.

In patients with acute lung injury (ALI) or acute respiratory distress syndrome (ARDS) in the Intensive Care Unit as well as in the operating room, a fluid therapy based on PPV monitoring has the following potentials: [1]

- Prediction of hemodynamic instability caused by positive end-expiratory pressure (PEEP)
- Prevention of excessive fluid restriction/depletion in patients with pulmonary edema
- Prevention of excessive ultra-filtration in critically ill patients undergoing hemo-dialysis or hemo-filtration
- Improvement of the outcome of patients undergoing high-risk surgery

Work Scope:

This thesis is based on a novel automatic algorithm introduced and improved by *M.Aboy*, that can be used to obtain the pulse pressure variation (PPV) from arterial blood pressure (ABP) signals [2]. The enhanced algorithm has been utilized, whereas the improvements to the first version [3] make it capable of estimating Pulse Pressure Variation during regions of abrupt hemodynamic changes and artifacts.

The aim of this report is to examine and compare the results of manually as well as automatically calculated pulse pressure variations to assess the agreement between $PPV_{(auto)}$ and $PPV_{(man)}$. Furthermore, to study the influence of tidal insufflations pressure on the capacity of pulse pressure variation (PPV) as a dynamic predictor of fluid responsiveness.

Thesis Outline:

The Introduction is followed by Chapter 2 with a Physiological Background addressed in this research.

The main goal is divided into two main parts which are discussed in chapter 3 and 4.

Chapter 3 gives complementary details about Pulse Pressure Variation and the implemented estimation algorithm. Algorithm assessment results are presented after and the chapter is ended by bringing the limitations of the implemented method in the Discussion part.

Chapter 4 deals with investigating the effect of intrathoracic pressure and/or tidal volume on the capacity of Pulse Pressure Variation. The chapter is followed by patient results on fluid challenge besides vasopressor challenge and is finalized by discussion on the capability of PPV in prediction of fluid responsiveness in patients.

Chapter 2 : Physiological Background

The Heart, a pump within a pump – two circulatory systems intertwined with the airways

The heart acting as a muscular organ holds the responsibility of receiving blood returned from the circulation and pumping the blood into the circulatory system by regularly recurring contractions. The heart can be considered as a pump with two interconnected circuits, the systemic sub serving vital organs such as kidney, liver, brain, intestines and lungs; and the pulmonary circuit leading deoxygenated blood from the systemic circulation to the lungs where it is oxygenated and further on pump it into the systemic circulation through the left-sided heart chambers. The two circuits have differing characteristics in terms of pressures: the systemic circulation is a high pressure system, whereas the lung circulation is working at low pressure. The heart performing as a “fluid” pump is a part of the systemic circulation. The whole pulmonary circulation is enclosed within an “air” pump, through the lungs.

The right side of the heart is responsible for receiving de-oxygenated blood during the diastolic period from the body (venous return (VR)) to the right atrium (RA) (via superior and inferior caval veins) , and further on pump it into the lungs via the right ventricle by contraction. This process is in order to exchange gas in the pulmonary vascular bed (Pulmonary circulation) [4]. From there, by means of the pulmonary veins, oxygen enriched blood from the lungs is gathered in the left atrium (left heart) during diastole. Partly, this blood flows directly into the left ventricle from the left atrium, a fraction, usually 50-60%, is pumped out into the systemic arteries (via the aorta) when the heart starts to contract. Finally the blood will end up in the systemic veins and enters the right heart again, this process closes the circulation.

With each beat a particular volume of blood is pumped from the ventricles of the heart, this is called stroke volume (SV). The stroke volumes of right and left ventricle are equal and only differ during short periods of equilibration. This is calculated by subtracting the volume of blood in the ventricle at the end of a beat, end-systolic volume (ESV), from the volume of blood just

prior to the beat, the end-diastolic volume (EDV). Cardiac output (CO) is the total volume of blood being pumped out of the ventricles beat per minute (mL blood/min).

Cardiac Output in mL/min = heart rate (beats/min) * stroke volume (mL/beat)

The cardiac output is the summation of the stroke volumes per minute with unit L/min [4].

Cardiac index (CI) is cardiac output normalized by the surface area of the patient (BSA) measured with units of L/min/m².

Cardiac output is uniquely determined by the efficiency of the heart and venous return. The efficiency of the heart is described by the Frank-Starling curve. Venous return is determined by the difference of pressure between the venous system (around 70% of blood volume) and the right atrium (RAP or CVP) and the resistance to venous return (RVR). The pressure of blood in the venous system, the systemic filling pressure (Pms), is determined by its volume and vascular tone in terms of compliance and resistance.

The Frank Starling Curve or cardiac function curve

The Frank Sterling Curve or cardiac function curve is a graph illustrating the relationship between the preload (plotted along the x-axis) and the cardiac output or stroke volume (plotted along the y-axis) (Figure 1). Preload is defined physiologically as the stretch of cardiac muscle fibres before contraction. Right arterial pressure (RAP) or pulmonary capillary wedge pressure (PCWP) are often used as a surrogate measure. From the above mentioned, it should be clear that preload is better represented by mean systemic filling pressure (Pms) subtracted by (RAP):

Preload=Pms -RAP

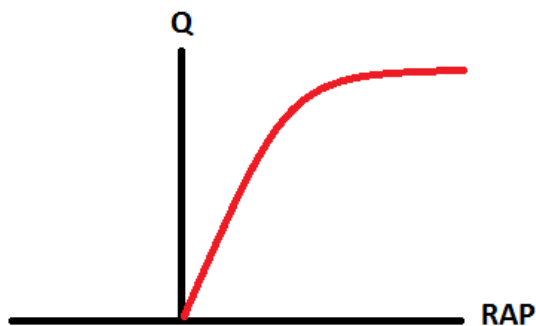


Figure 1 Cardiac function curve .The diagram illustrates the Frank–Starling law of the heart; the Y axis describes the stroke volume or cardiac output (mL/min). The X axis describes end-diastolic volume, right atrial pressure, or pulmonary capillary wedge pressure (mm Hg).

Venous Return

Two curves are illustrated in Figure 2:

Cardiac Function Curve: This is the Frank-Starling curve for the ventricle showing the relationship of cardiac output as a function of right arterial pressure (RAP).

Venous Return Curve: This curve shows the relationship between blood flow in the vascular system -venous return- and right arterial pressure (RAP).

The point where the venous return curve intersects the X axis is addressed as Mean Systemic Filling Pressure (Pms). When there is 'no flow' in the system, the mean systemic pressure (Pms) reflects the right arterial pressure (RAP). At this point the pressure is equal throughout the circulatory system.

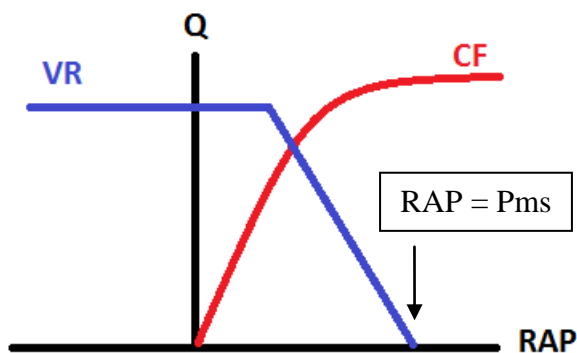


Figure 2 Simultaneous plots of the cardiac and vascular function curves. The two curves cross at the point of equilibrium for the cardiovascular system. The Y axis describes the stroke volume or cardiac output (mL/min). The X axis describes right arterial pressure (mm Hg). As flow, Q, approaches zero, (RAP) approaches (Pms) which by definition is the pressure in the vascular system at zero flow. It is realized at heart arrest and ventricular fibrillation.

The Y-axis position of the venous return is evidently dependent on the volume-cum-pressure of the venous system. This and the pressure drop from the venous circulation to right atrium. This pressure difference is affected by the cyclic positive pressure insufflation of the lungs which *reduces* the pressure difference and thus venous return. The reduced venous return during insufflation results in a diminished right ventricle stroke volume (RV SV). Conversely, during exsufflation the pressure differences (Pms-RAP) increases and thus the (RV SV). The stroke volume (SV), whether produced during insufflation or exsufflation , passes the pulmonary circulation and present themselves after 2-3 heartbeats (often cited in literature, but no

explanation given to the numbers) to the left heart chambers. This series of smaller/larger SVs produced at respiratory rate theoretically may arrive at left heart in or out of synchrony with respiration. The insufflation pressure “squeezes” blood from the pulmonary circulation into the left side of the heart and thus add a small volume which will increase stroke volume (SV), whether of the smaller or the larger variety, and this SV is then ejected by the left ventricle (LV) into the circulation which for the sake of the argument can be assumed to have a constant compliance.

The principle of superposition may be applied to waves whenever two (or more) waves travelling through the same medium at the same time. It is important to consider the wave reflection between incident pressure wave ejected from the heart and reflected pressure wave caused by insufflations pressure. The two forenamed waves travelling in the same direction could have either constructive or destructive interference.

The venous volume may be changed in a number of ways. The obvious way is to volume resuscitate the patient, another would be to mobilize fluid from unstressed to stressed volume (the concept of stressed/unstressed volume will be no further elaborated in this context) and yet another way would be for the excursions in respiratory pressure to “squeeze” blood from the pulmonary circulation into the left side of the heart and thus add a small volume which will increase stroke volume (SV). Focusing on this last mechanism it is evident that patients operating on the flat portion of the Frank–Starling curve are insensitive to cyclic changes in preload induced by mechanical inspiration, meaning that PPV is low (Figure 4).

Conversely, PPV is high in patients operating on the steep portion of Frank–Starling curve .It means that mechanical inspiration could cause cyclic changes which can manipulate blood volume (Figure 3). Whether moving toward steep or flat portion of the curve can help predicting fluid responsiveness in patients.

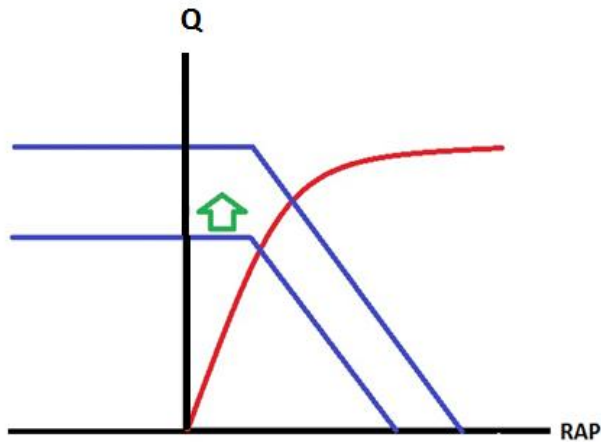


Figure 3 Simultaneous plots of the cardiac and vascular function curves or venous return curve. The two curves cross at the point of equilibrium for the cardiovascular system the Y axis describes cardiac output (mL/min). The X axis describes right arterial pressure (mm Hg). PPV is high moving toward the steep portion of the curve.

As to the effect of insufflation pressure on right ventricle stroke volume (RVSV) and its transmission through pulmonary circulation, it is evident that the smaller the pressure difference (Pms-RAP) is, as a consequence of the venous volume, the greater the relative reduction in pressure difference caused by the positive pressure insufflation will be, and – all things equal – the greater the effect on the left sided SV and consequently on the arterial pressure amplitude.

Conversely, PPV is high in patients operating on the steep portion of the preload/stroke volume relationship and hence sensitive to cyclic changes in preload induced by mechanical inspiration (Figure 3).

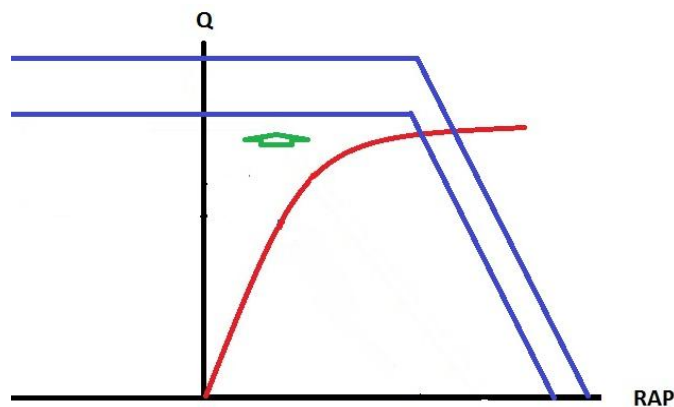


Figure 4 Simultaneous plots of the cardiac and vascular function curves or venous return curve. The two curves cross at the point of equilibrium for the cardiovascular system the Y axis describes cardiac output (mL/min). The X axis describes right arterial pressure (mm Hg).

The mean systemic pressure (Pms) is affected by the blood volume as well as venous compliance. Changes in the mean systemic pressure (Pms) will shift the venous return curve towards left or right.

Cardiac output may increase or decrease by altering the Frank-Starling curve, the venous return curve, (Figure 5), or both. An increase in blood volume and/or a decrease in venous compliance increases the mean systemic pressure (Pms). This will act as a means to shift the vascular function curve to the right, illustrating an increase in both cardiac output (CO) and right arterial pressure (RAP). (Figure 4) shows the simultaneous plots of the cardiac and venous return curve and the shift of (Pms) to the right.

On the contrary, mean systemic pressure (Pms) is decreased by a decrease in blood volume and/or an increase in venous compliance. This will shift the vascular function curve to the left, illustrating a decrease in both cardiac output (CO) and right arterial pressure (RAP) .

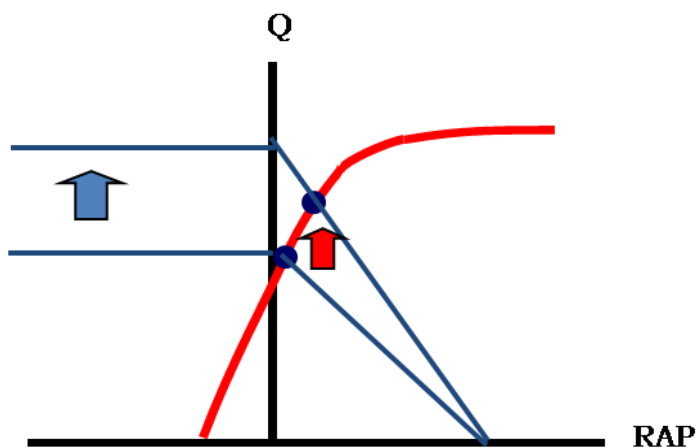


Figure 5 Simultaneous Plots of the cardiac and vascular function curves or venous return curve. The effect of resistance to venous return on cardiac output is demonstrated.

The Cardiac Cycle

The diastolic filling of the heart is related to the temporal course of the cardiac cycle as well as the pressure/volume relations between venous system and right sided heart chambers. The cycle, as stated, is divided into two fundamental phases: diastole and systole [4]. The first phase is diastole, which represents a brief period just prior to filling (the ventricles are relaxing) and the

ventricular filling per second. The second stage is systole, which represents the time of contraction and ejection of blood from the ventricles [5]. The important observation for the present thesis is that left ventricle (LV) filling (stages 5-7 in figures) is following an exponential course. Filling, thus, is time dependent and the marker of time is the heart rate.

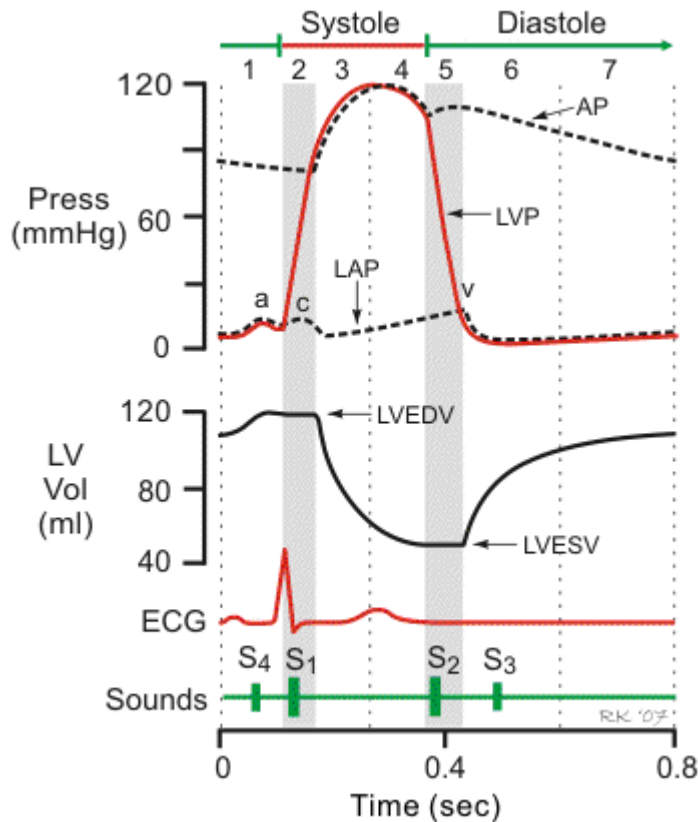


Figure 6 Arterial Blood Pressure in relation to the pressure and the volume in the left ventricle. LV stands for left ventricle, LA stands for left atrium, LVEDV stands for left ventricular end diastolic volume and LVESV for left ventricular end systolic volume[6].

Figure 6 illustrates seven phases as well as a plot of the aortic pressure together with the pressure and volume in the left ventricle to give an idea of how these pressures relate to each other and to the volume in the left ventricle. These phases are briefly mentioned below: [5]

Phase 1 - Atrial Contraction

Phase 2 - Isovolumetric Contraction

Phase 3 - Rapid Ejection

Phase 4 - Reduced Ejection

Phase 5 - Isovolumetric Relaxation

Phase 6 - Rapid Filling

Phase 7 - Reduced Filling

In summary it may be concluded that changes in preload induced by cyclic changes in intrathoracic pressure may lead to changes in pulse pressure dependent on the patient's position on the Frank-Starling cardiac function curve. It is further hypothesized that changes in pulse pressure are related to the size of changes in intrathoracic pressure. It could also be added that heart rate dependent ventricular filling may be reflected in pulse pressure variations as well.

Chapter 3 : Pulse Pressure Variation Estimation

3.1 Introduction

3.1.1 Pulse Pressure variation

The arterial pulse pressure variation (PPV) induced by mechanical ventilation has been found to be one of the most accurate and specific predictors of fluid responsiveness in patients [7].

Pulse Pressure (PP) is defined as the difference between systolic pressure and diastolic arterial pressure. Maximal PP (PP_{max}) and Minimal PP (PP_{min}) are calculated over a single respiratory cycle. Additionally it has been observed that (PP_{max}) is always featured during the inspiratory period, while (PP_{min}) occurs during the expiratory period.

The factors affecting PPV have been described above. It however, uses the variation in pulse pressure ($P_{systolic} - P_{diastolic}$) caused by inspiration and expiration (equation 1).

$$PPV(\%) = \frac{PP_{max} - PP_{min}}{\frac{PP_{max} + PP_{min}}{2}} * 100$$

Equation 1

(PP_{max}) : pulse pressure where the pulse pressure is at its maximum

(PP_{min}) : pulse pressure where the pulse pressure is at its minimum

It is very important to point out that Pulse Pressure Variation (PPV) is not an indicator of the volume status, nor a marker of cardiac preload, but is an indicator of the position on the Frank–Starling curve to predict fluid responsiveness [1].

PPV can be utilized to predict the hemodynamic effects of blood loss as well as fluid loading. In other words a large PPV or an increase in PPV can be interpreted as operating on the steep

portion of Frank-Starling curve warning the responsible physician to counteract further fluid depletion to avoid hemodynamic instability [8].

3.1.2 Pressure Pulse Morphology

The pulse morphology of the ABP signal is well known and consists of a percussion peak, dichrotic notch and dichrotic peak [9]. Figure 7 shows an example of an ABP signal and its components.

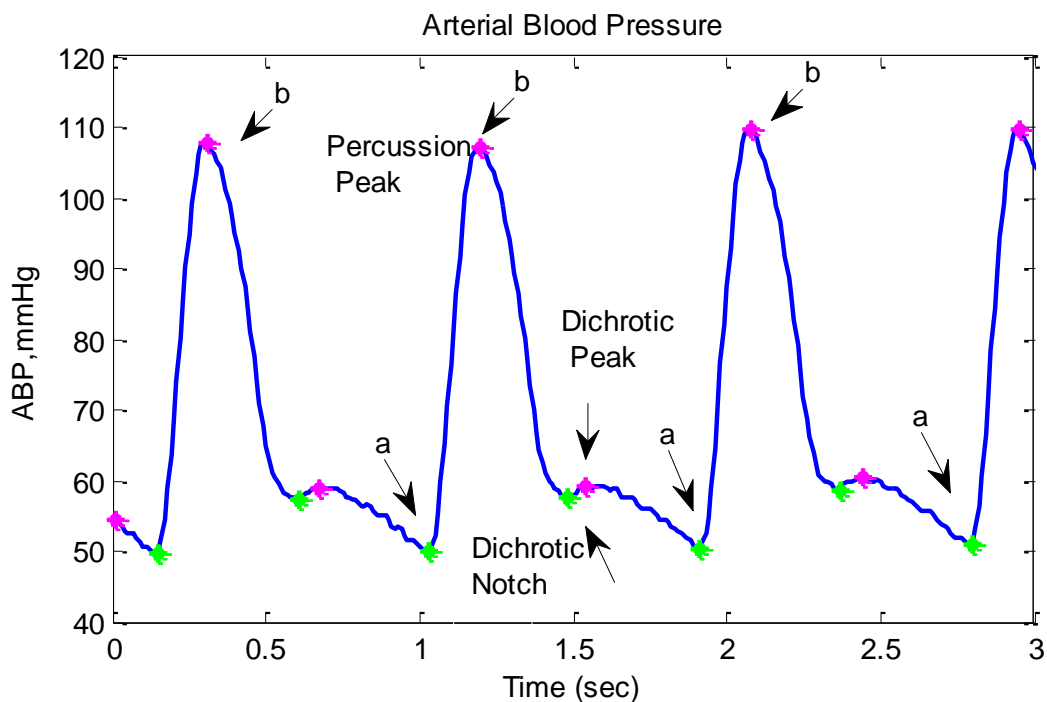


Figure 7 Arterial Blood Pressure waveform components. Percussion peak, Dichrotic notch and Dichrotic peak are marked.

3.2 Algorithm Description

The algorithm presented in four steps is programmed in MatlabR2009B. These steps can be briefly represented as:

Step 1: Beat Detection and Segmentation

Step 2: Beat Maxima Detection

Step 3: Envelope Estimation

Step 4: PPV Estimation

The Pulse Pressure Variation algorithm utilizes an automatic beat detection algorithms to sense each beat. This could be either ABP or plethysmographic beat. Next pulse pressure (PP) is calculated in each beat and upper and lower envelopes of pulse pressure variation are estimated. PP time series is calculated by subtracting upper and lower envelopes. The Pulse pressure signal is searched for maxima and minima within each respiratory cycle and minimal and maximal PP are derived in each cycle to estimate PPV.

3.2.1 Step 1: Beat Detection and Segmentation

Almost all the physiologic signal detection algorithms can be divided into two stages. Figure 8 contains a block diagram that outlines a *pre-processing stage* to extract the desired components in order to maximize the signal-to-noise ratio (SNR) and a *decision stage* which determines if an incoming peak is a true component based on a user-specified threshold. Traditional algorithms in the pre-processing stage are employed using signal feature extraction and digital filters [10] while recent algorithms utilize wavelets and filter banks for pre-processing [11][12].

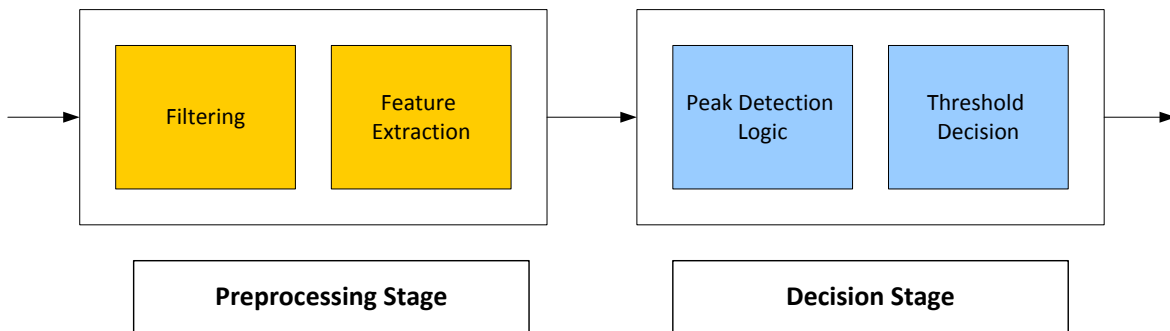


Figure 8 Block diagram of common structure of detection algorithms

Figure 8 explicitly illustrates a block diagram of the implemented detection algorithm. It is divided into two stages as it was mentioned earlier.

The Pre-processing Stage: All the peaks are detected in the raw signal prior to any filtering. The pressure signal is pre-processed by the Digital Filtering unit along side with Maxima/Minima Detection unit which consists of two Low-pass and High-pass elliptic filters with different cut-off frequencies. The output of the filters is used to estimate the heart rate based on the estimated power spectral density (PSD).

The Decision Stage: Peak detection and decision logic are based on rank-order (percentile-based) nonlinear filters, which incorporate relative amplitude and slope information to coarsely estimate the percussion and systolic peak components. Since rank based filter detection results are made on the filtered signal, there must be a nearest neighbour algorithm to compare the peaks in the raw signal and the detected components in the filtered signal to validate the location of **(a)** and **(b)** components as shown in (Figure 7).

Ultimately, the Interbeat Variability Classification stage combines the classification results together with the estimated heart rate to find components in the arterial blood pressure signal.

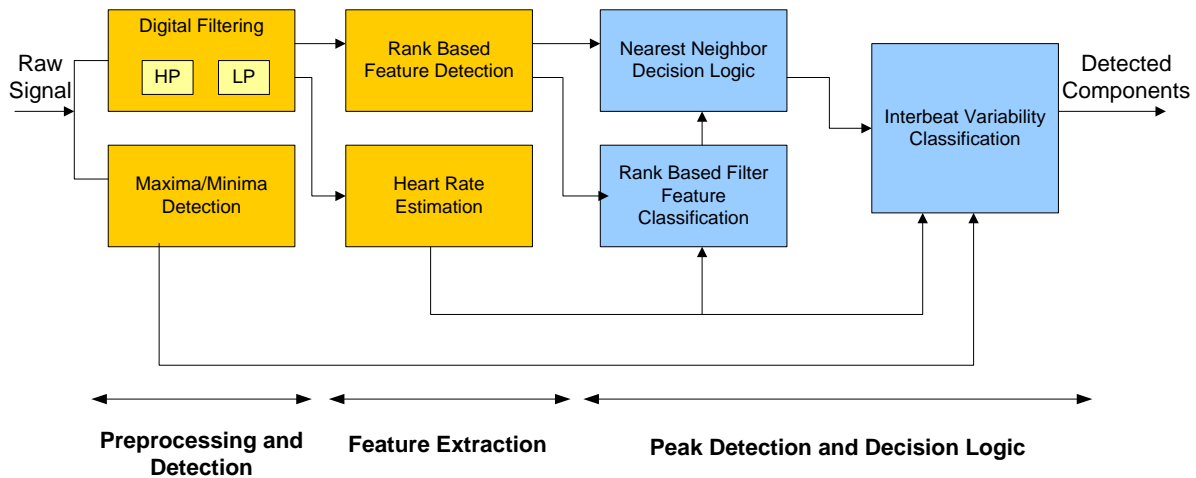


Figure 9 Block diagram of the architecture of detection algorithm

An automatic beat detection algorithm described in [10] is employed to detect beats in Arterial Blood Pressure (ABP).

This beat detection algorithm identifies the time-location of the systolic peak in ABP which is the first peak following each heartbeat. The algorithm finds minima (preceding each beat) which are the time location of the start of each beat,

$$\mathbf{a} = (a_1, a_2, \dots, a_N)$$

The ABP signal is segmented into N vectors based on the vector \mathbf{a} by the beat detection system which implies N individual beats in the signal. The beat segmentation process is essential in extracting ABP features.

3.2.1.1 Maxima/Minima Detection

The algorithm detects all the maxima and minima in the arterial blood pressure signal prior to any filtering.

The minima and the maxima points are defined as:

$$Xmin = x(n): x(n - 1) > x(n) < x(n + 1) \quad \text{Equation 2}$$

$$Xmax = x(n): x(n - 1) < x(n) > x(n + 1) \quad \text{Equation 3}$$

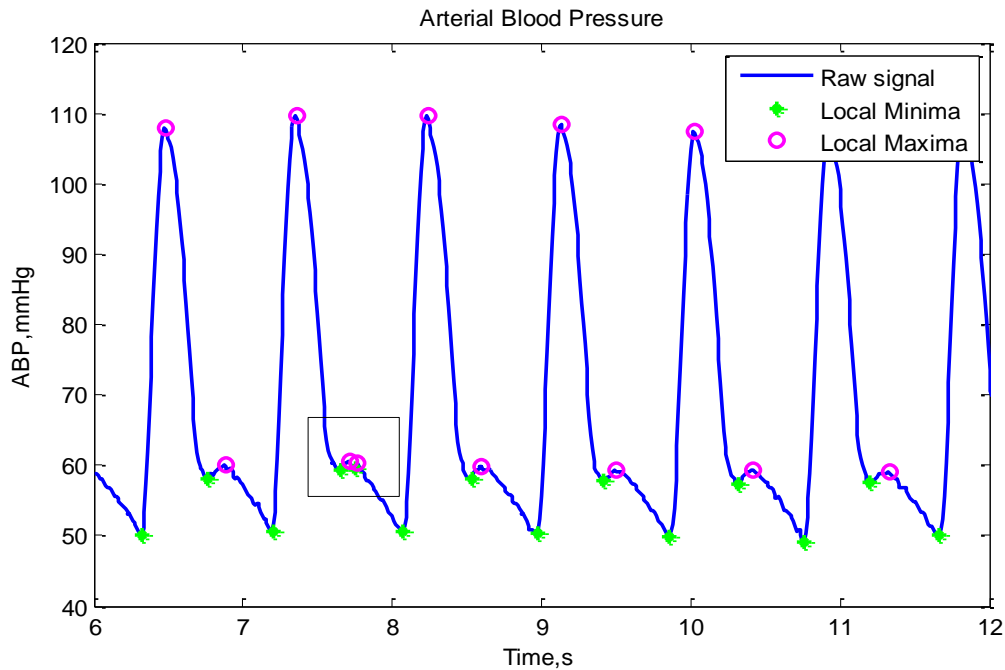


Figure 10 Waveform components –maxima and minima- on an ABP signal. Maxima and Minima are marked by ‘o’ and ‘*’.

The detected peaks will be used later on to correct the output results from rank based feature classification unit in the Inter-beat Variability (IBI) classification unit. Figure 10 illustrates the local maxima and minima in ABP signal marked by ‘o’ and ‘*’ respectively.

As it can be seen in Figure 10 there exist some false detection for both maxima and minima. That implicitly clarifies the necessity of filtering the pressure signal. Moreover, in some cases filtering results which is discussed in pre-processing stage are not satisfactory. Regarding the trade-off between optimality and practicality the appropriate band pass filtering is not capable of filtering out the noise in such a way that the algorithm performs robustly. To avoid such a problem an adjustment to the implemented algorithm by M.Aboy et al. [2] is made so that the Maxima and Minima results are fed into Rank Filter Classifier unit to resolve the detected components.

3.2.1.2 Pre-processing Stage

The pre-processing stage consists of two elliptic filters. The first High-pass filter removes the signal trend. Since most of the power in a human pressure signal is above 0.7 Hz [12], the low cut-off frequency is selected to be 0.5 Hz. The next Low-pass filter is designed to smooth the signal and eliminate high frequency noise that might interfere with the onset detection of the arterial blood pressure (ABP). The high cut off frequency is 7.5 Hz. Both Low-pass and High-pass filters are fifth-order generated by MATLAB©. The signal is band-pass filtered with zero phase delay and then utilized to estimate the heart rate (HR) in the next step.

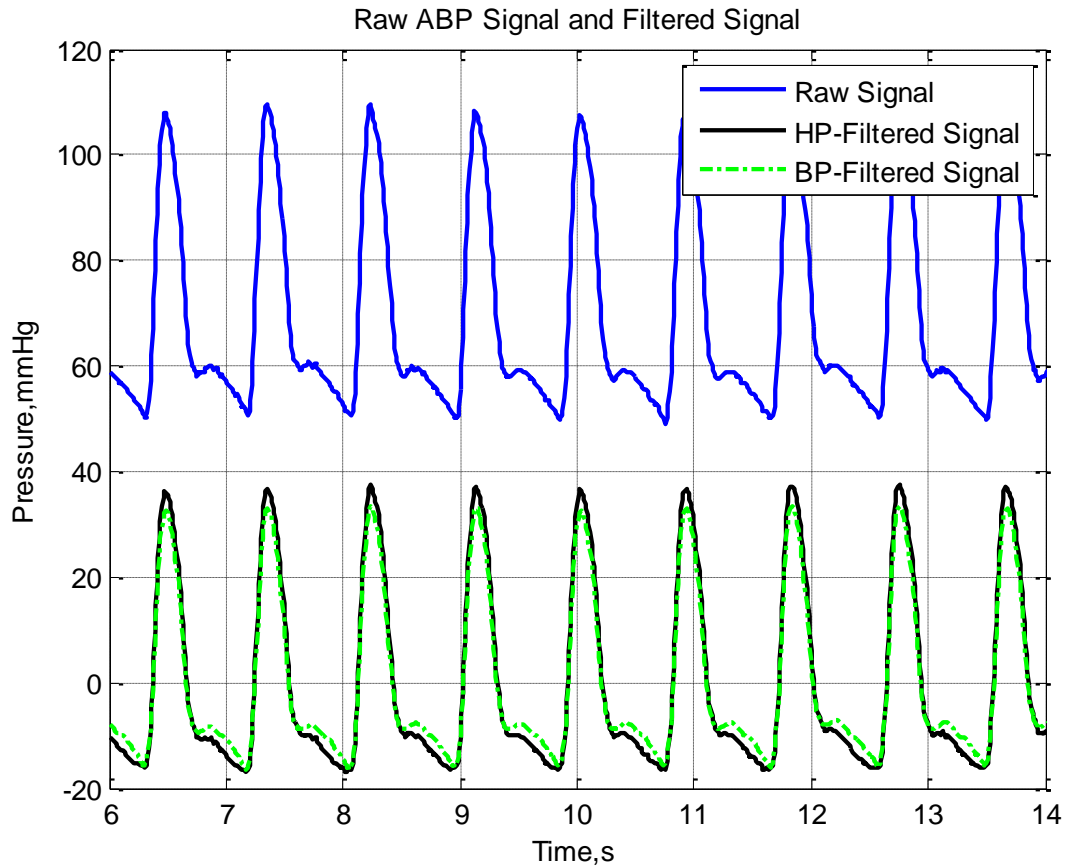


Figure 11 The raw blood pressure signal (blue curve) and Hp filtered signal in black curve as well as Band Passed filtered signal in green which is the result of High and Low pass filtering are illustrated in the figure.

3.2.1.3 Spectral Heart Rate Estimation

At this stage, the filtered pressure signal is divided into 10 second non overlapping windows. *Power Spectral Density* (PSD) is estimated in each partition by using the Blackman-Tukey method. The algorithm seeks the frequencies where the PSD is maximum. The frequency component with the largest magnitude - highest power - is assumed to be the heart rate of each window.

The average inter-beat interval (AVR IBI) is estimated from the median of the inverse heart rates, where derived from each of the 10 second windows. In order to avoid artifacts in the windows the median filter is utilized [11].

$$AVR\ IBI = median \{1/f_1, 1/f_2, \dots, 1/f_w\}$$

Equation 4

f_i : Heart rate frequency in i^{th} window

3.2.1.4 Peak Detection based on Rank Filter Classification

Rank Filter Classification

The pressure signal which is band-passed filtered in the pre-processing step is then fed into a rank-based filter to detect the peaks in each signal partition. As covered before, rank filter is applied likewise to the detected maxima and minima in the raw signal. The rank based filter detects a components in both unprocessed and filtered signal (as shown in Figure 12 and Figure 13) alike b components (as shown in Figure 14 and Figure 15)

The maxima and minima components can be introduced as:

$$a = X_{min} < 20thpercentileinawindow$$

Equation 5

$$b = X_{max} > 75thpercentileinawindow$$

Equation 6

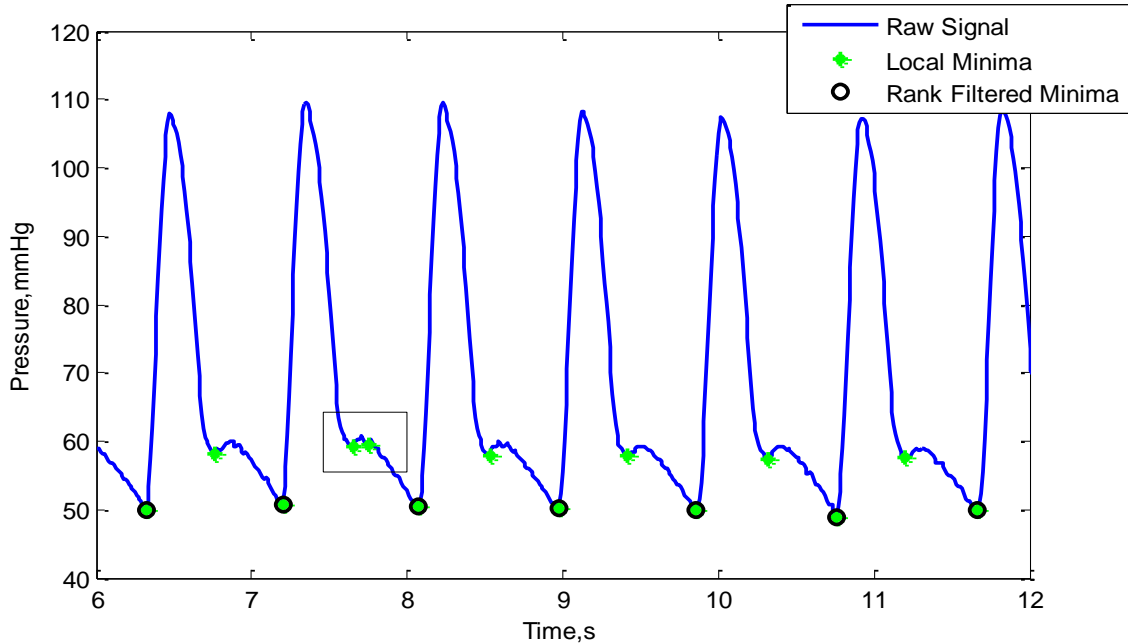


Figure 12 Rank Order Filter Classification results on the raw signal -Local minima which are shown by ‘*’ and minima extracted based on Rank Order filtering marked by ‘o’.

Local minima are illustrated with ‘*’ although there exist some over-detection in a number of beats which are removed by rank-order filter .The results are marked by ‘o’ in the figure. A similar filtering has been applied in order to resolve maxima and the peaks are presented with ‘o’ in(Figure 14).

(Figure 12) and (Figure 13) below the 20th percentile and in (Figure 14) and (Figure 15) above the 80th respectively, are classified by using a running window of 10 seconds.

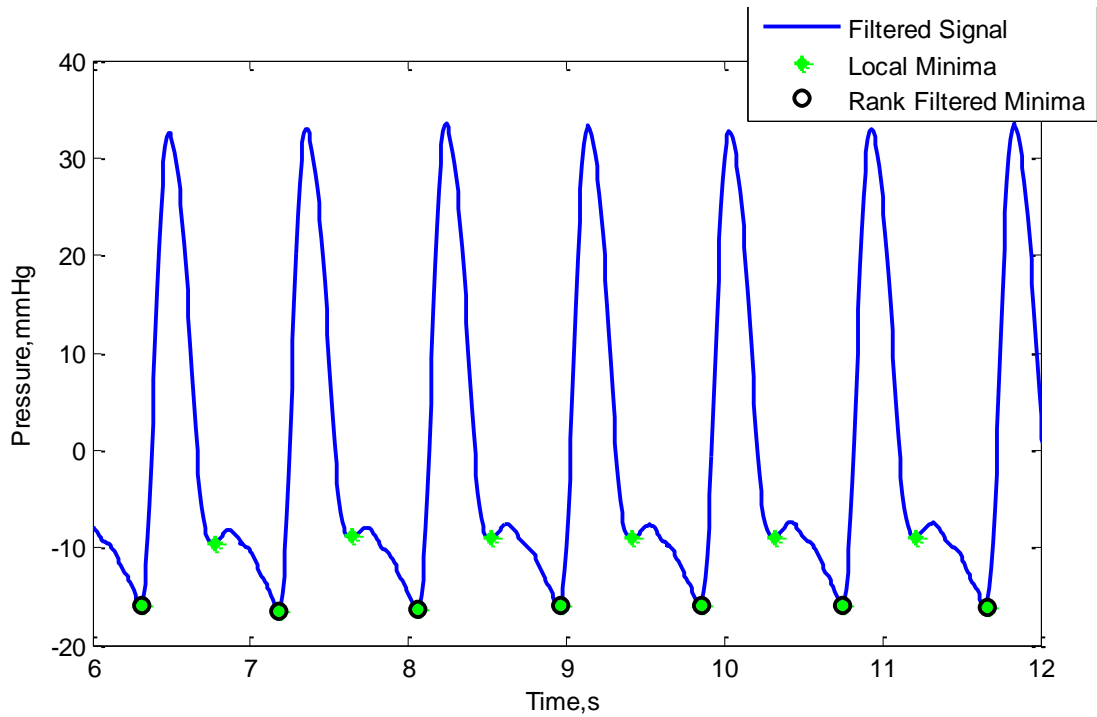


Figure 13 Rank Order Filter Classification results on the filtered signal. Rank Filter is applied to the filtered signal. Local minima and Rank Order filtered minima are marked by '*' and 'o' respectively.

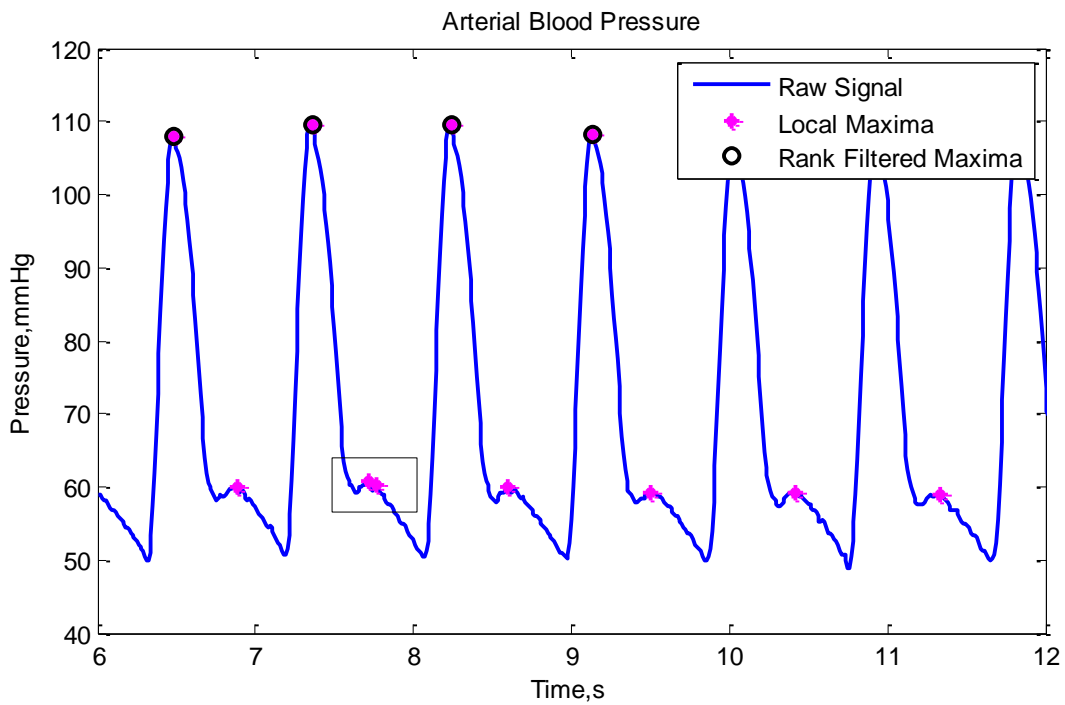


Figure 14 Rank Order Filter Classification results on the raw signal. Rank Filter is applied to the filtered signal. Local maxima and Rank Order filtered maxima are marked by '*' and 'o' respectively.

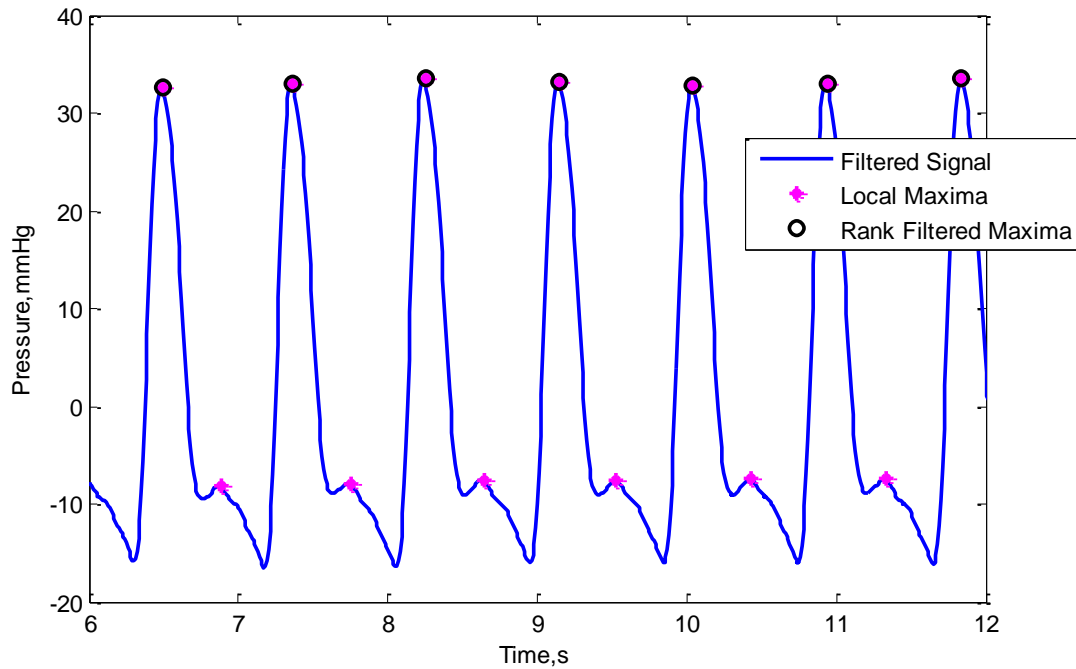


Figure 15 Filtered Signal Rank Order Filter Classification results .Rank order filter is applied to the filtered signal. Local maxima and Rank filtered maxima are marked by ‘*’ and ‘o’ respectively.

3.2.1.5 IBI Classification Logic

Rank based filter results are two time series corresponding to b as maxima and a as minima which contain inter-beat intervals between the location of the maxima and minima components. The actual time interval between individual beats of the mammalian heart is defined as Inter-beat Interval (IBI). The aim of this step is to remove the false positives (FP) where the detector has over-detected a component and false negatives (FN) whenever the detector has missed it. (AVR IBI) is calculated, which can be put to be used as a scale to discover overlooked detections as false negatives (FN) and over detections as false positives (FP).

During a recursive search process whenever the inter-beat distance is lower than $AVR/2$ (false positive), the component must be removed and the time series must be reconstructed. Similar search processes, look for the cases where the inter-beat distance is greater than $2*AVR$ (false negative).

The time series are searched for cases where the inter-beat distance is less than $0.75*AVR$ and $1.75 *AVR$ which are over-detection and misdetections respectively.

In order to get rid of detecting possible misdetections and over-detections within heart rate limits two rank-order filters at the 90th and 10th percentile are applied to the corrected IBI series

As obtained in pre-processing stage, two time series of maxima and minima exist which are employed to correct the problem. In order to find the appropriate location of the peaks, the algorithm imports the components from initial maxima and minima time series (pre-processing results) that minimize the inter-beat variability.

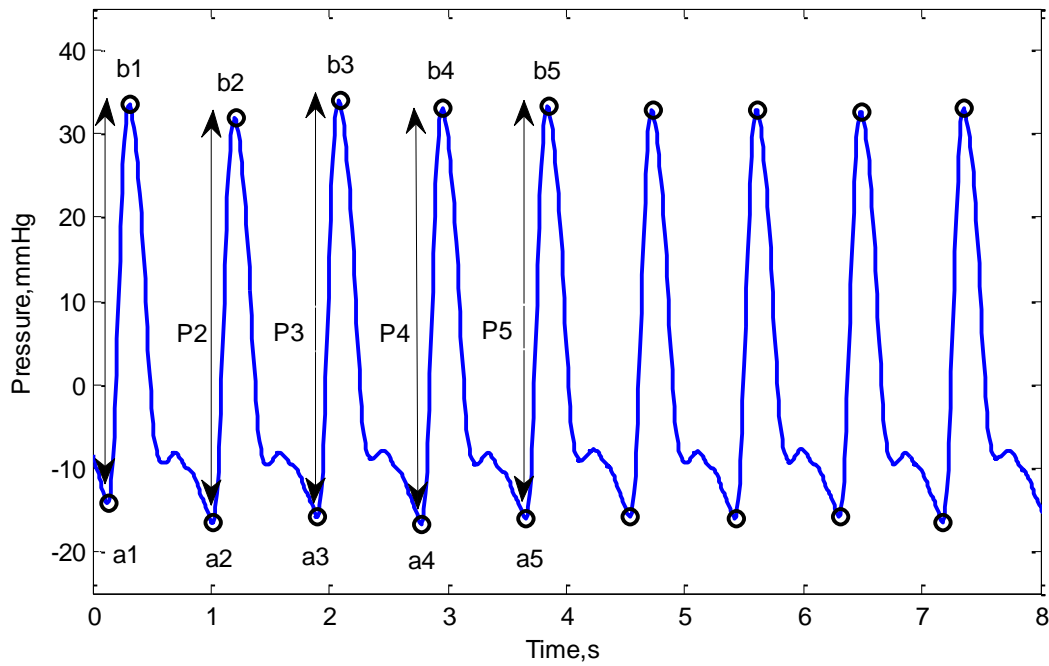


Figure 16 Automatic Beat Detection. $a_i = (a_1, a_2, \dots, a_N)$ are sample indices corresponding to the beginning of each beat and $b_i = (b_1, b_2, \dots, b_N)$ are sample indices relative to the maxima of each beat.

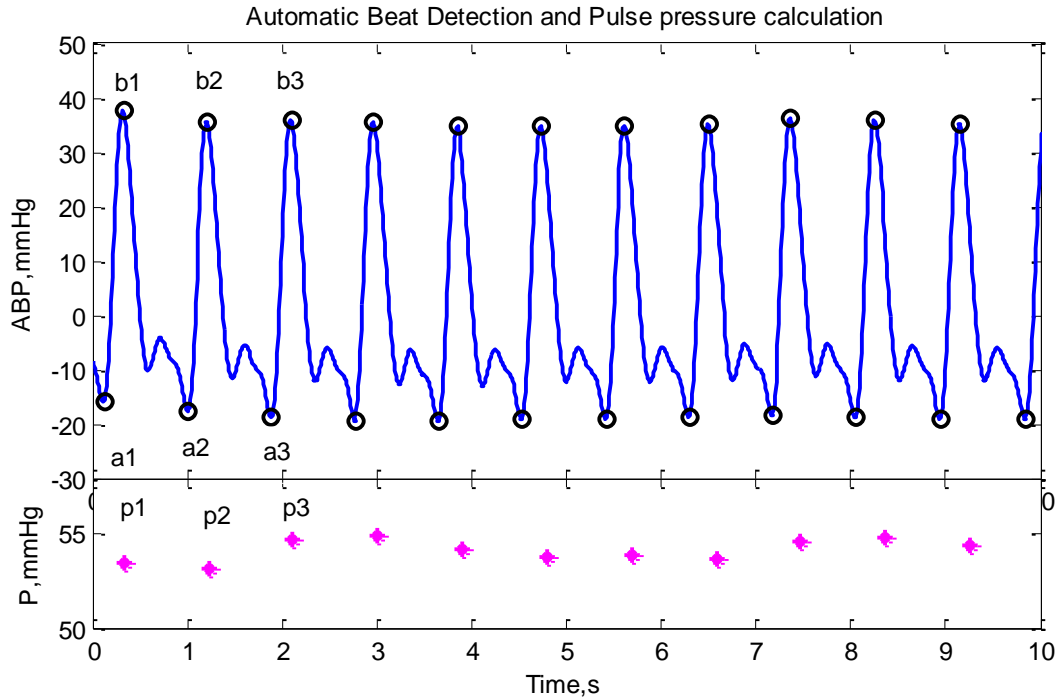


Figure 17 Step 1. Automatic Beat Detection and pulse pressure calculation.

3.2.2 Step 2: Beat Maxima Detection

The beat detection algorithm as discussed earlier finds the maxima in the pressure signals. Given the segmented signal (starting with each minimum) a maxima vector \mathbf{b} can be introduced as it contains the sample indexes corresponding to the maxima of each beat.

3.2.3 Step 3: Envelope Estimation

In this step $x(\mathbf{a})$ and $x(\mathbf{b})$ time series are exploited to estimate Lower $l(n)$ and Upper $u(n)$ envelopes respectively. Gaussian kernel is practiced among popular kernels used for smoothing the foresaid time series.

Recalling that the Gaussian kernel is defined as:

$$K(x, y) = \exp\left(\frac{-\|x - y\|^2}{2\sigma^2}\right)$$

Equation 7

A clipped Gaussian kernel function characterized as below is used

$$b(u) = \begin{cases} \exp\left(\frac{-u^2}{2}\right) & u < |5| \\ 0, & otherwise \end{cases} \quad \text{Equation 8}$$

By means of a kernel smoother, $x(\mathbf{a})$ and $x(\mathbf{b})$ time series are smoothed and re-sampled at a rate of sampling frequency of ABP [2].

$$u(n) = \frac{\sum_1^N x(\mathbf{b}) b\left(\frac{|nTs-t(k)|}{\sigma}\right)}{\sum_1^N b\left(\frac{|nTs-t(k)|}{\sigma}\right)} \quad \text{Equation 9}$$

$$l(n) = \frac{\sum_1^N x(\mathbf{a}) b\left(\frac{|nTs-t(k)|}{\sigma}\right)}{\sum_1^N b\left(\frac{|nTs-t(k)|}{\sigma}\right)} \quad \text{Equation 10}$$

$Ts = 1/fs$	Re-sampling Interval(corresponding with sampling frequency of ABP)
$t(k)$	Times of signal observation
σ	Kernel Width

For heart rates up to 4 Hz a kernel width (σ) of 0.2 seconds is appropriate.

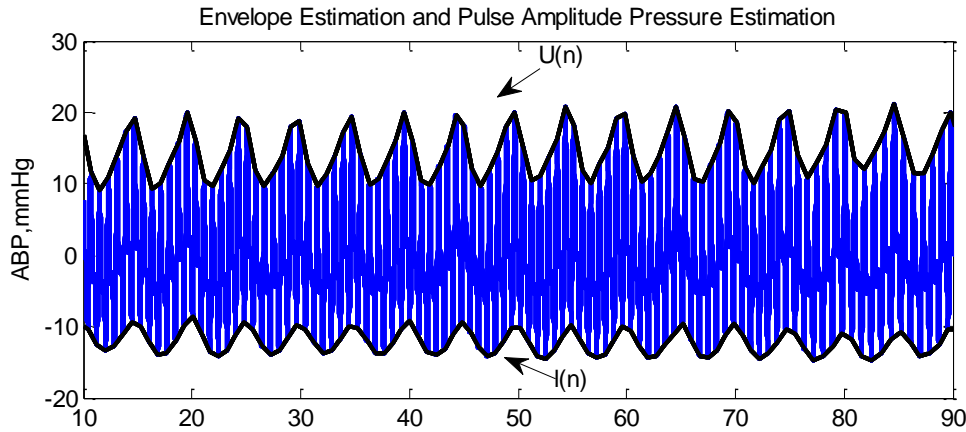


Figure 18 Upper and Lower Envelope Estimations are presented by $u(n)$ and $l(n)$ respectively.

An estimate of the pulse amplitude for each beat can be calculated by subtracting estimated upper and lower envelopes.

$$PP = u(n) - l(n)$$

Equation 11

3.2.4 Step 4: PPV Estimation

The pulse pressure variation (PPV) is estimated from PP time series. The PP signal is subdivided into 50% overlapping vectors in order to accurately find the maxima and minima in PP time series. The dimension of the vectors depends on the respiratory frequency which is directly calculated from the Pulse Pressure estimation that also represents as respiratory signal. In other words Maximum PP_{max} and Minimum PP_{min} pulse pressures are determined over the same respiratory cycle. PPV in each respiratory cycle is calculated according to Equation 1

$$PPV(\%) = \frac{PP_{max} - PP_{min}}{\frac{PP_{max} + PP_{min}}{2}} * 100$$

3.3 Methods: Algorithm Assessment

3.3.1 Beat Detection

Algorithm Validation

The algorithm's performance in Peak Detection was assessed using ABP dataset publicly available online at <http://bsp.pdx.edu> which has provided annotated examples for developers. The flagged peaks by Expert DT were employed to be the gold standard against the algorithm prediction.

Benchmark Parameters

Association for the Advancement of Medical Instrumentation (AAMI) has provided two benchmark parameters to assess the algorithm's performance: Sensitivity (Se) as an indicator of the percentage of the true beats that was correctly detected, and Positive Predictivity (+P) as the percentage of detected beats that were tagged by the expert as well. These two are defined as:

$$Se = \frac{TP}{TP + FN} \quad \text{Equation 12}$$

$$+P = \frac{TP}{TP + FP} \quad \text{Equation 13}$$

TP: number of true positives: detected true peaks

FP: number of false positives: detected false peaks

FN: number of false negatives: non detected true peaks

Table 1 validates the performance of the algorithm by illustrating the Sensitivity (Se) as well as Positive predictivity (+P).

ABP	Sensitivity (%)	Positive Predictivity (%)	FN	FP
Abp1	99.86	99.25	8	43
Abp2	99.97	99.72	2	21

Table 1 Validation of the Algorithm’s Performance compared to the professional annotation of two ABP signals. Sensitivity and Positive Predictivity (in percent) are calculated in order to quantify the performance.

3.3.2 PPV Estimation

Data Recording:

Arterial blood pressure signal was recorded from Datex-GE invasive pressure module to a personal computer using Datex-GE proprietary data acquisition software. Collect ver. 4.

Statistical Data Analysis

In order to assess the performance of the implemented automatic PPV estimator algorithm, PPV_{auto} –algorithm results- were compared against a commercial functional hemodynamic monitoring system LiDCO plus (LiDCO Ltd, Cambridge ,United Kingdom). PPV_{auto} is calculated and averaged over four respiratory cycles of five seconds each.

In order to analyse the agreement between results a Bland-Altman plot is exercised. This difference plot implies that any two methods that are implemented to measure the same parameter (or property) will have a good correlation in a selected set of samples.

During Bland-Altman analysis the limits of agreement are computed usually in the form as *bias* $\pm (1.96 \sim 2) STD$ (average difference ± 1.96 standard deviation of the difference).

Agreement between PPV_{LiDCO} and PPV_{auto} (Bland Altman analysis) is 0.58 ± 1.31 (Figure 19 and Figure 20) over 110 pairs of data.

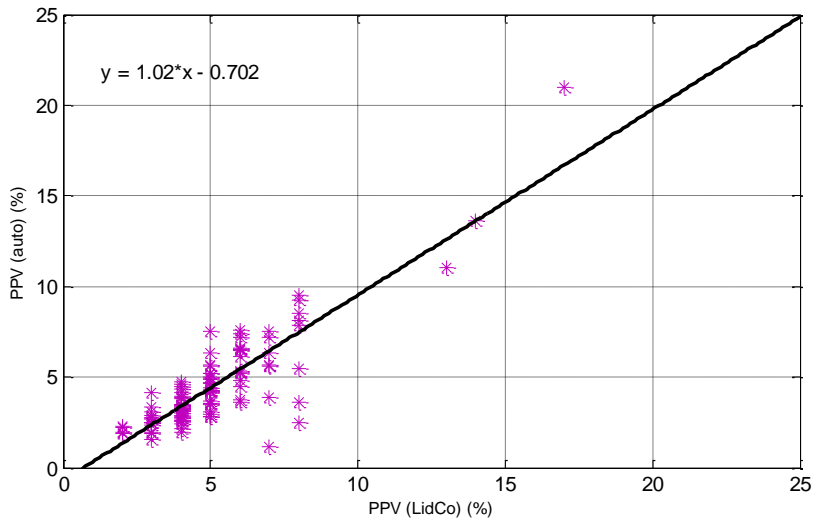


Figure 19 Relationship between PPV_{LidCo} and PPV_{auto}

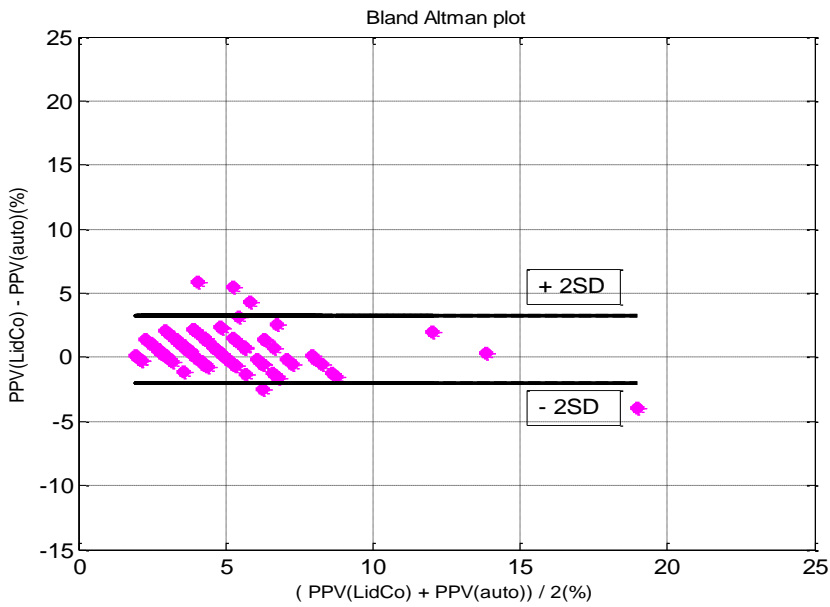


Figure 20 Bland Altman analysis for PPV_{LidCo} and PPV_{auto}. Agreement between PPV_{LidCo} and PPV_{auto} is 0.58 ± 1.31 .

Chapter 4 : Evaluation of the influence of tidal insufflations pressure on the capacity of pulse pressure variation (PPV) to predict fluid responsiveness.

4.1 Introduction

Recently, studies show that great potential arise from PPV in fluid management and hemodynamic optimization.

Several factors most likely influence PPV that some of them are verified during the experiment:

Volume challenge:

Volume Expansion (VE) is known as one of the possible alternatives to improve hemodynamics in the patients, notwithstanding the fact that immoderate VE cause fluid accumulation, which may be hazardous. Consequently, fluid responsiveness prediction is highly demanded in patients. [13]. Volume can be in form of blood products, colloid, or crystalloid.

Vasoactive Challenge:

Vasoactive therapy drugs can be categorized as vasodilator, vasoconstrictor or inotropes. In this study vasoconstrictor challenge is in the form of increase of epinephrine, or phenylephrine infusion. Vasoconstrictors produce constriction of the blood vessels and a consequent rise in blood pressure.

4.2 Methodology

4.2.1 Patient Study

Patients were studied perioperatively during major surgery. During stable operative phases, tidal volume (the breath volume of air mixed with anaesthetic gases insufflated into the patient's lungs) was varied from 5 to 7 to 9 mL/kg and recordings were made of arterial and airway pressure at 100 Hz. The patient study is based on two distinct experiments on an orthopaedic patient and the other one on a bariatric patient.

4.2.2 Animal Study

This study could help comparing effects on PPV at different PEEP levels and between different ventilation modes (conventional and High Frequency Jet Ventilation (HFJV)). The animal study is followed in three steps and the results of different PEEP level are manifested in eleven stages. These three steps can be summarized as:

- Baseline
- After Lavage (washing)
- After Recruitment Manoeuvre

4.3 Results

4.3.1 Patient Study Results:

Patient 1) Orthopaedics Patient

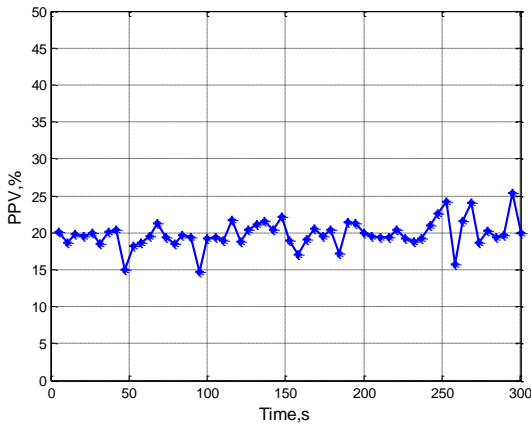
Fluid challenge as well as the vasopressor (vasoconstrictor) challenge was the major goal of this experiment. Before and after fluid challenge, complete hemodynamic measurements including PPV were obtained.

In the processing of stages 1-3 the aim is to examine the relationship between Pulse Pressure Variation (PPV) and intrathoracic pressure variation considered as Minute Volume variations (MVV), while in stages 5-8 the relationship between PPV and volume expansion is going to be analyzed. There are several approaches for volume expansion. Among them the blood was administered as well as colloid. In stage 1 The MVV increases from 6.5 L/min to 7.5 L/min in stage 2 and then decrease to 5.5 L/min in stage 3. Subsequently MV=5.5 L/ min is set to be the baseline before volume resuscitation. In stage 4, volume resuscitation with first colloid is considered. In stage 5, blood is used to resuscitate the volume. In the 6th and 8th stage the second and third portions of 500 ml of colloids are consumed. The measurement period for the proceeding stages (4,5,6,8) are 20 minutes period which the PPV measurement is determined after 10 minutes in order to consider hemodynamic stability. Stage 7 is also considered to study the effect of a vasoconstrictor 'Phenylephrine' injection during the Volume resuscitation process. PPV and $PPV_{(mean)}$ which is averaged over four respiratory cycles of five seconds is calculated and corresponding figures are projected into Figure 21 through Figure 28. Figure 21-Figure 23 demonstrates different Tidal Volumes and measured PPV. Figures 24 -28 illustrates the effect of vasopressor challenge on PPV.

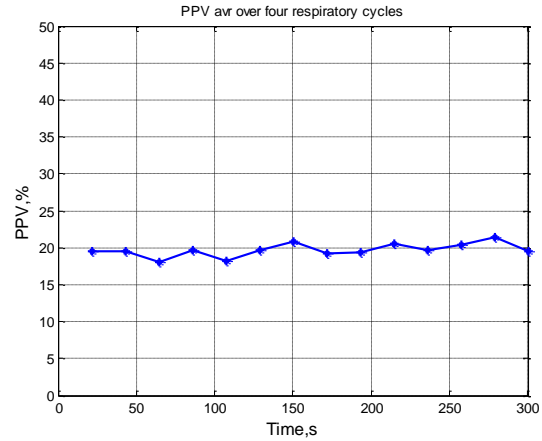
For the figures 21-47 (a) represents PPV value and (b) shows PPV_{mean} as the PPV average over four respiratory cycles. As it can be seen in some proceeding plots some figures contain abrupt sudden peaks which cannot be explained by any physiological reasoning, but only considering the fact that the data may be corrupted by artifacts ("noisy" physiological environment) since it has been collected during surgical operation where it is difficult to obtain stable conditions when performing singular interventions. (i.e Figure 28). Although filtering help retrieving the real data

out of noisy one but there is always a trade-off between filtering and keeping the main data which imply that artifacts are inevitable.

Stage 1: MV 6.5 L/min



(a)

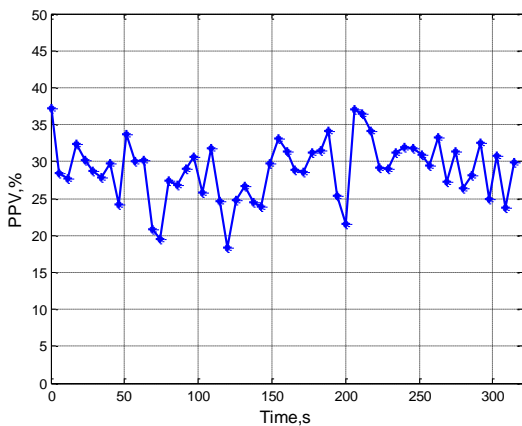


(b)

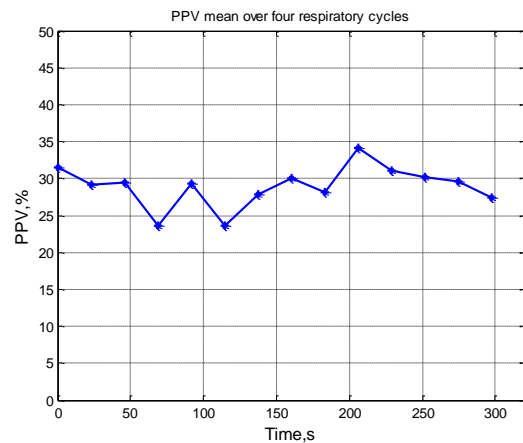
Figure 21 PPV is represented in (a) likewise PPV mean over four respiratory cycles for MV 6.5 L/min in b.

The patient study started at Minute volume = 6.5 L/min and increased to 7.5 L/min in stage 2. It was expected that increment cause increase in PPV and the result approved the theory. PPV (mean \pm SD) varied from (19 ± 4) to (28 ± 2) .

Stage 2: MV 7.5 L/min



(a)



(b)

Figure 22 PPV and PPV mean over four respiratory cycles for MV 7.5 L/min are represented in a and b respectively.

By increasing the volume we increase the intrathoracic pressure, therefore we block the blood returning to the heart, which may cause increment in the PPV.

Stage 3: MV 5.5 L/min

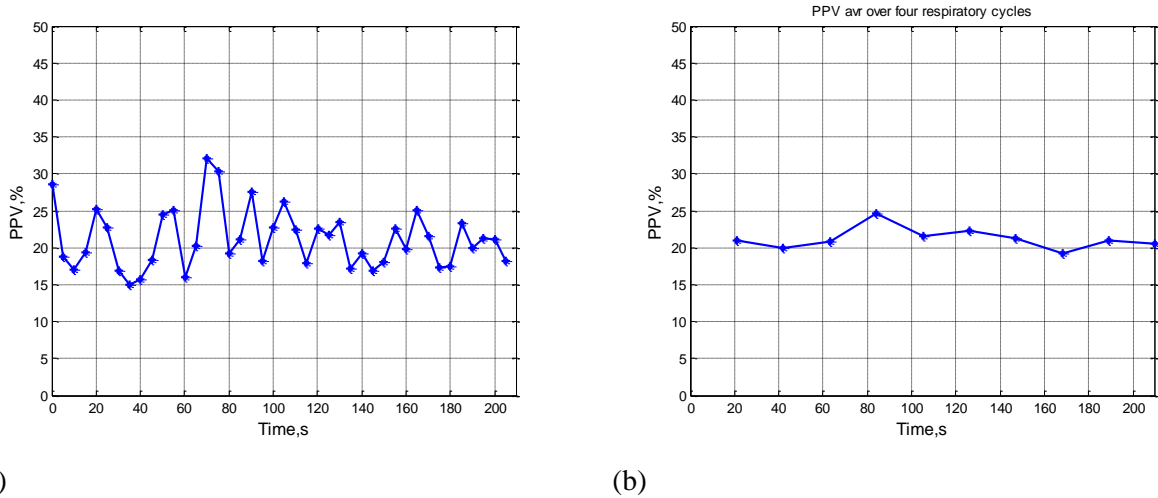
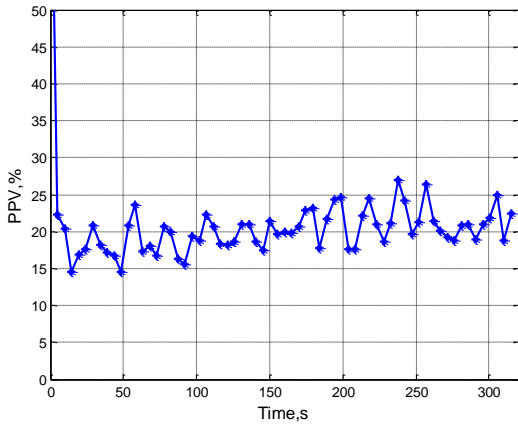


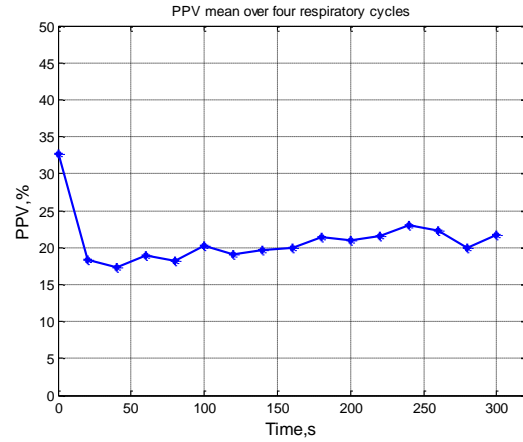
Figure 23 PPV and PPV mean over four respiratory cycles for MV 5.5 L/min are represented in a and b respectively.

The decrement takes place in two major steps, one from 7.5 to 6.5 and the other from 6.5 to 5.5. It was predicted that lowering the MV to 5.5 L/min would cause decrement in PPV, however the reduction was less than expected from (28 ± 2) to (22 ± 2) . PPV values for MV challenge as well as Fluid challenge are displayed in Table 2 and Table 3 respectively.

Stage 4: First 500 ml colloid MV 5.5 L/min



(a)



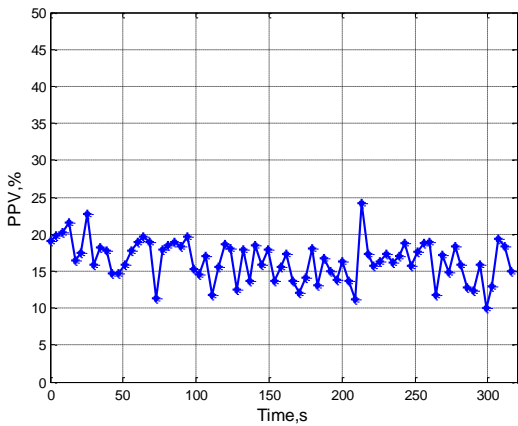
(b)

Figure 24 PPV and PPV mean over four respiratory cycles after 1st volume expansion are represented in a and b respectively.

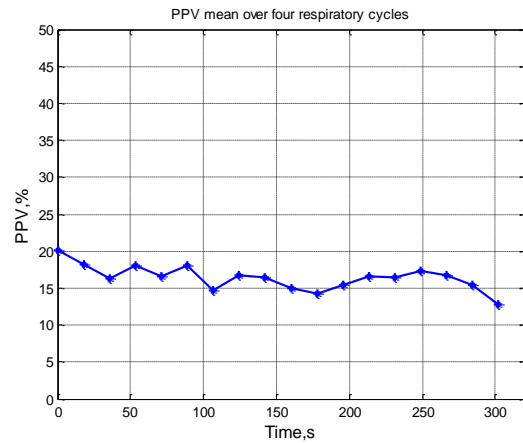
Volume challenge results are manifested in stages 4, 5, 6 and 8 and PPV is in a decreasing order.

VE results are displayed in figures 24, 26, 28 and 28.

Stage 5: Blood Volume



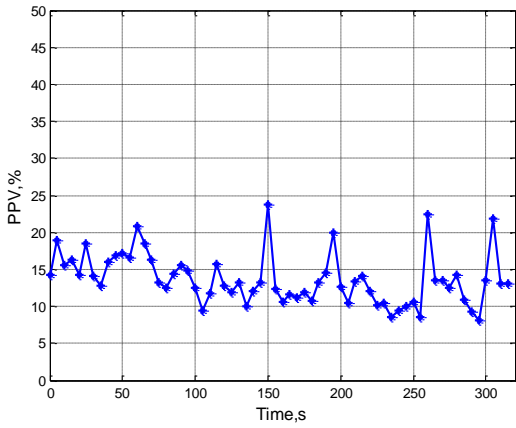
(a)



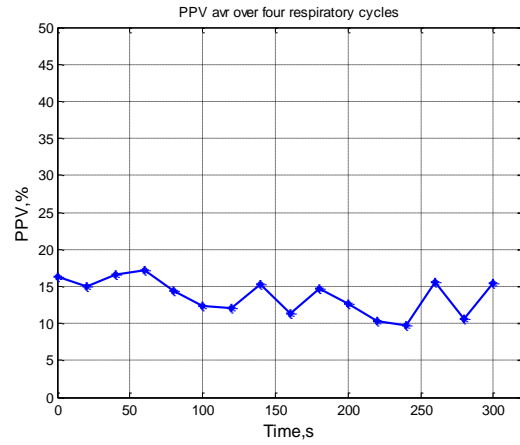
(b)

Figure 25 PPV and PPV mean over four respiratory cycles 2nd first volume expansion are represented in a and b respectively.

Stage 6: Second 500 ml of colloid



(a)

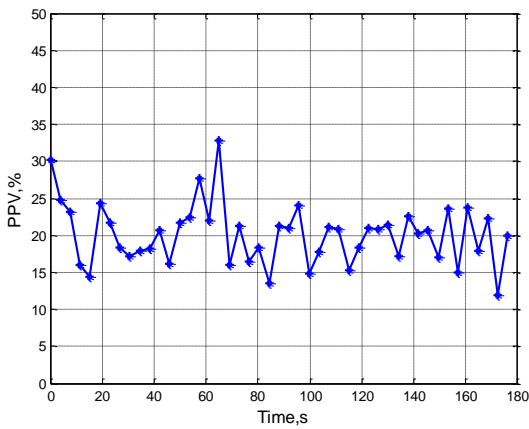


(b)

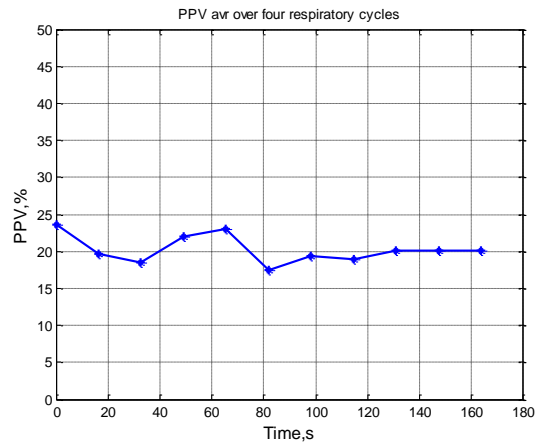
Figure 26 PPV and PPV mean over four respiratory cycles after third volume expansion are represented in a and b respectively.

Stage 7: Phenylephrine Injection

Phenylephrine acts as an agent to increase blood pressure. Due to clinical condition of the patient Phenylephrine was administered which as a vasoconstrictor cause higher blood pressure and accordingly higher PPV is expected. The result is displayed in Figure 27.



(a)



(b)

Figure 27 PPV and PPV mean over four respiratory cycles are represented in a and b respectively.

Stage 8: Third 500 ml of colloid

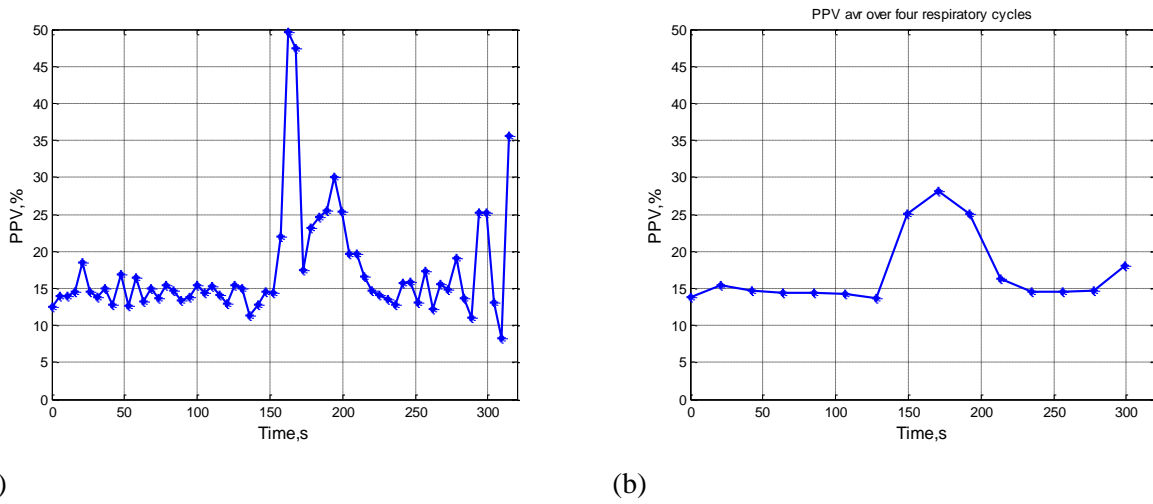


Figure 28 PPV and PPV mean over four respiratory cycles after 4th volume expansion are represented in a and b respectively.

In this part Fluid challenge results along with MV challenge effects on PPV are discussed. The relationship between Pulse Pressure Variation and Minute Volume Variation are shown in Table 2. Pulse pressure variation results due to volume expansion interventions are illustrated in Table 3.

MV Variation	Mean ± SD	Mean ± SD (Averaged over 4 respiratory cycle)
MV 6.5 L/min	19±4	19± 0.9
MV 7.5 L/min	28 ± 10	28 ± 2
MV 5.5 L/min	21 ±7	21 ± 1

Table 2 MV Challenge: Relationship between PPV and MVV.

Volume Expansion	Mean \pm SD	Mean \pm SD(Averaged over 4 respiratory cycle)
1st colloid	20 \pm 7	20 \pm 1
Blood	16 \pm 6	16 \pm 1
2nd colloid	13 \pm 6	13 \pm 2
Phenylephrine	20 \pm 8	20 \pm 1
3rd colloid	17 \pm 6	17 \pm 4

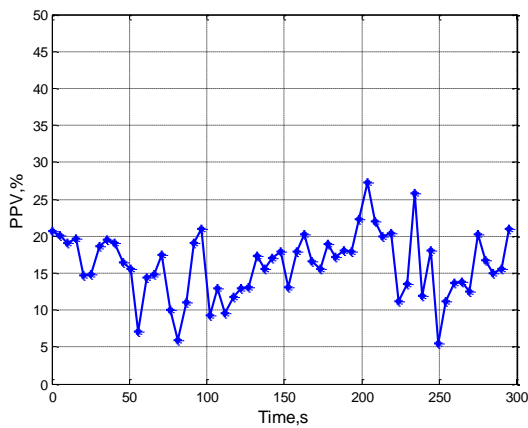
Table 3 Fluid Challenge: Relationship between PPV and VE.

Patient 2) Bariatric Patient

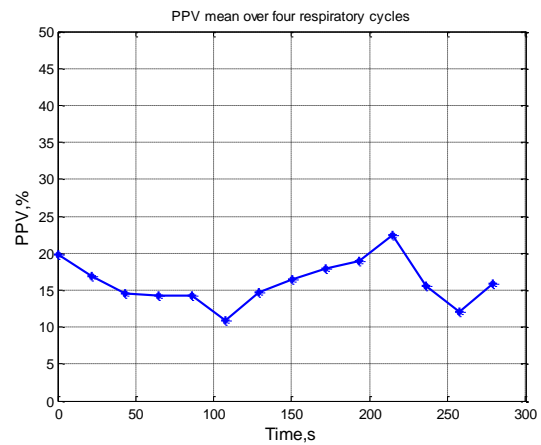
The first stage is perceived as the period before the patient was put to sleeping state, which is so-called "pre-anaesthetic". Then there is a series of measurements at three increasing minute volumes (MV) 5.8, 6.6 and 7.4 L/min and a series of pre-, per and post infusion of 500 (mL) of colloid which are considered in stages (2, 3, 4, 5, 6, 7) and finally in stage 8 the data recorded during the period, when the patient woke up from anaesthesia, is examined. The pre infusion was defined as the time before starting infusion, per infusion was considered as time during infusion and post infusion was known as the time after treatment. It was supposed that the first and last recording illustrate the effect of abolishing sympathetic stimulation during induction of anaesthesia and the re-emergence of sympathetic stimulation during awakening.

PPV and $PPV_{(mean)}$ which is averaged over four respiratory of five seconds is calculated and corresponding figures from the Pre-anaesthetic stage to Post-op are manifested into Figure 29 through Figure 36. PPV values are presented in Table 4.

Stage 1 :Pre-anaesthetic



(a)

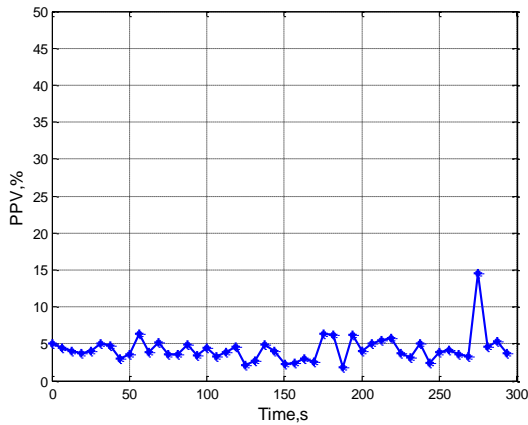


(b)

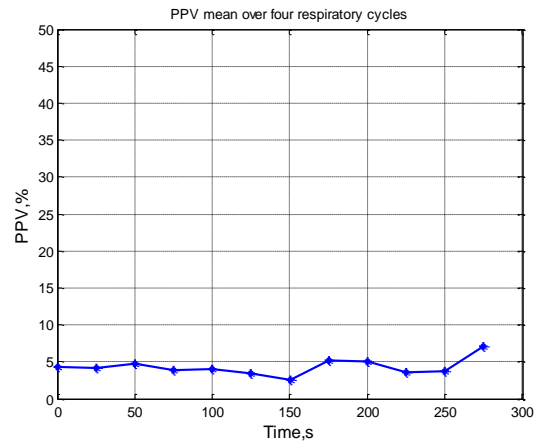
Figure 29 Pre-anaesthetic stage : PPV and PPV mean over four respiratory cycles are represented in a and b respectively.

Stages 2 to 4 deal with Minute Volume challenge. Volume was reinforced from 5.8 to 6.6 and PPV boosted the same way. Presumed behaviour should have figured for next volume rise, yet results do not abide by the anticipated order.

Stage 2: MV 5.8 L/min



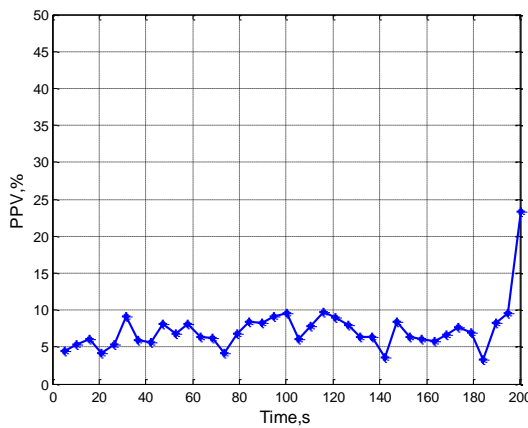
(a)



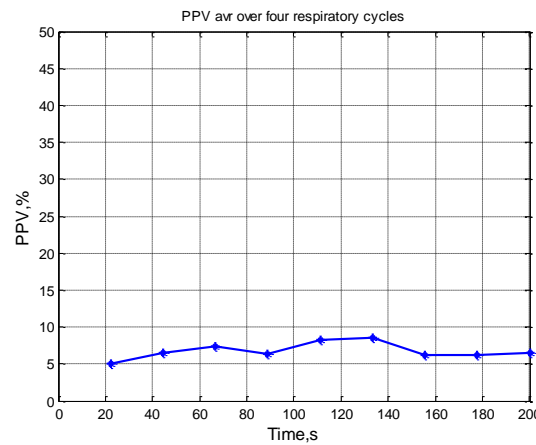
(b)

Figure 30 Fluid challenge: MV 5.8 L/min .PPV and PPV mean over four respiratory cycles are represented in a and b respectively.

Stage 3: MV 6.6 L/min



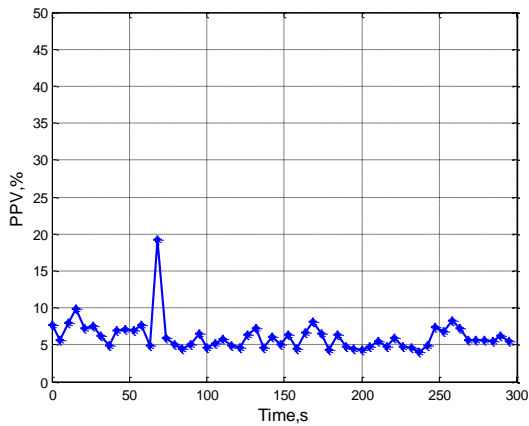
(a)



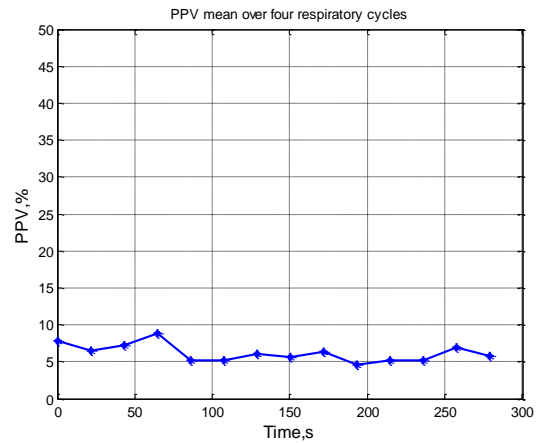
(b)

Figure 31 Fluid challenge: MV 6.6 L/min. PPV and PPV mean over four respiratory cycles are represented in a and b respectively.

Stage 4: MV 7.4 L/min



(a)

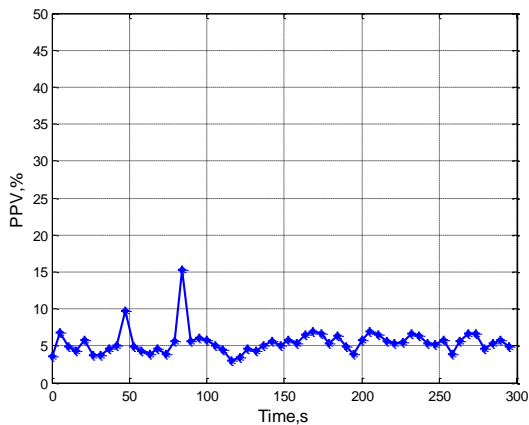


(b)

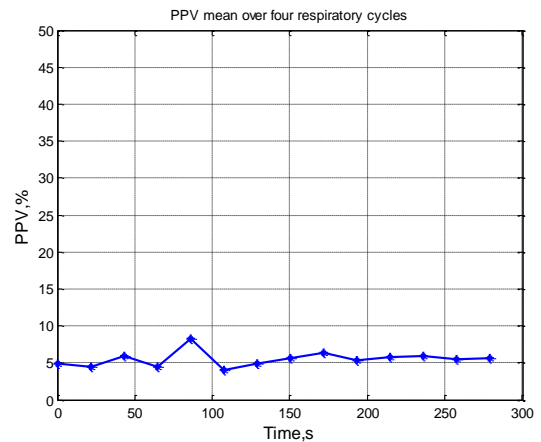
Figure 32 Fluid challenge: MV 7.4 L/min. PPV and PPV mean over four respiratory cycles are represented in a and b respectively.

Figure 33 displays PPV in baseline and Figures 34 and 35 show PPV for per infusion of 500 ml colloid and post infusion. As presumed colloid result in decrement in PPV which is in agreement with the results presented in Table 4.

Stage 5: Pre Infusion



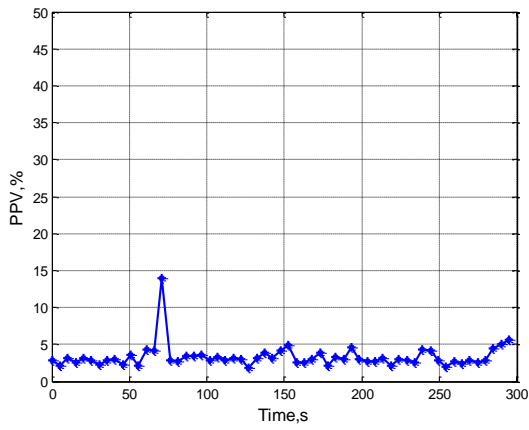
(a)



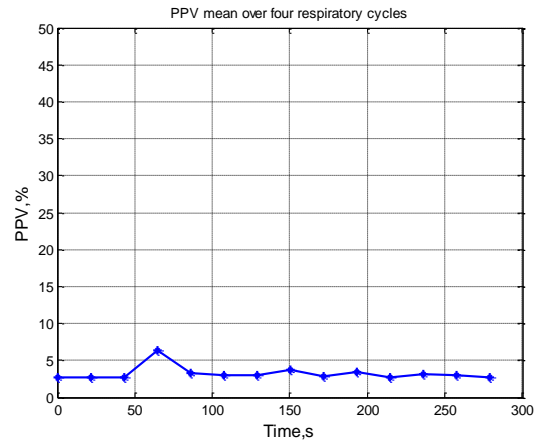
(b)

Figure 33 Pre-infusion of colloid PPV and PPV mean over four respiratory cycles are represented in a and b respectively.

Stage 6: Per Infusion (500 ml colloid)



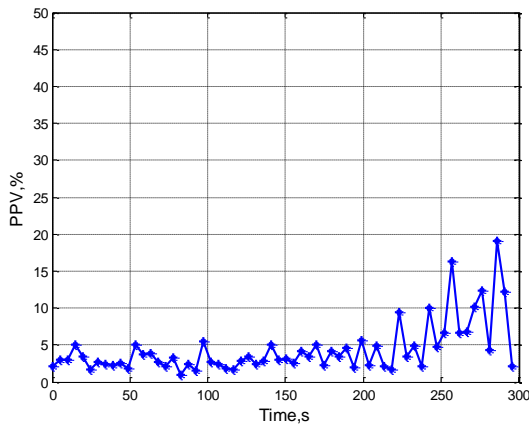
(a)



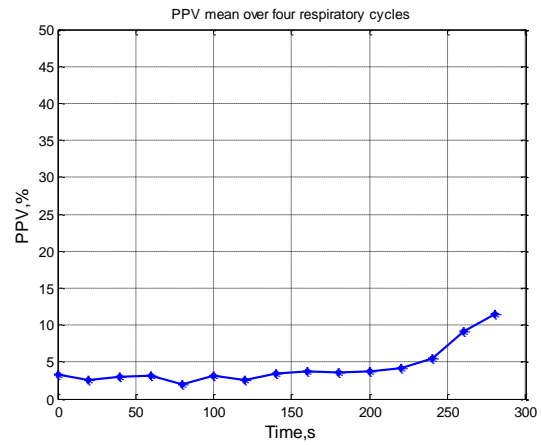
(b)

Figure 34 Vasopressor challenge: per infusion .PPV and PPV mean over four respiratory cycles are represented in a and b respectively.

Stage 7: Post Infusion



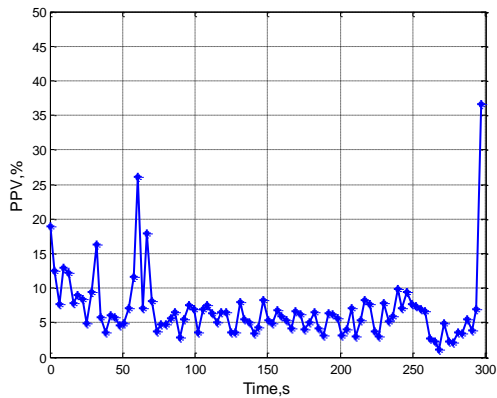
(a)



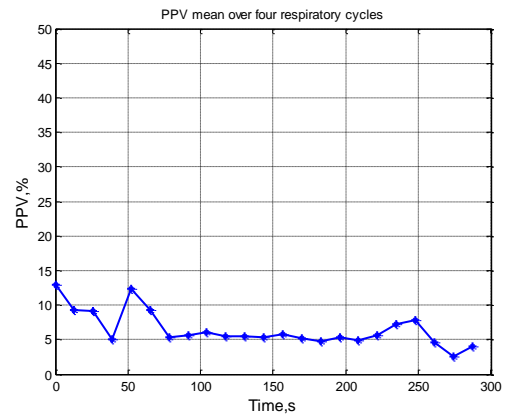
(b)

Figure 35 Post Infusion stage : PPV and PPV mean over four respiratory cycles are represented in a and b respectively.

Stage 8: Post Operation



(a)



(b)

Figure 36 Post Operation stage : PPV and PPV mean over four respiratory cycles are represented in a and b respectively.

The results for Patient 2 are shown in Table 4. As it was expected from, 5.8 L/min MV to 6.6 L/min there was an increase in PPV and PPV_{mean} , but from 6.6 L/min to 7.4 L/min there exists no change in PPV mean.

	Mean \pm SD	Mean \pm SD (Averaged over 4 respiratory cycle)
Pre-anaesthetic	16 \pm 6	16 \pm 3
MV 5.8 L/min	4 \pm 7	4 \pm 1
MV 6.6 L/min	7 \pm 3	6 \pm 1
MV 7.4 L/min	6 \pm 6	6 \pm 1
Pre-Infusion	5 \pm 2	5 \pm 1
Per-Infusion	3 \pm 1	3 \pm 0.9
Post-Infusion	4 \pm 6	4 \pm 2
Post-operation	6 \pm 5	6 \pm 2

Table 4 Variation in PPV in different staged during surgery (From Pre-anaesthetic to Post-operation).

4.3.2 Animal Study Results

In the introduction of the experiment the animal was ventilated with a conventional ventilator at PEEP 5 cm H₂O, which is considered as the Baseline (BL).

Next, the lungs are washed with saline to remove surfactant; this makes the lungs very stiff and prone to collapse. In stage two a recording with normal ventilator at 5 cm H₂O PEEP.

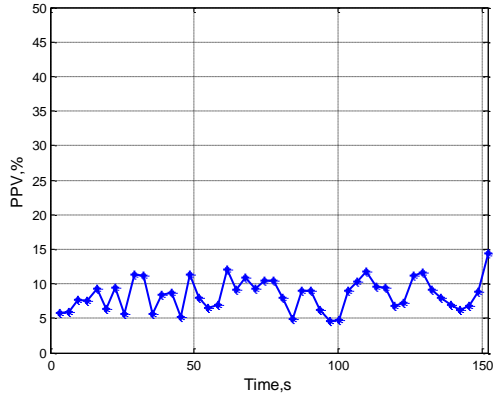
Subsequently, the recruitment manoeuvre starts that lung is recruited using high pressure for short periods of time. By means of a special ventilator which operates at TWO frequencies. One frequency is 20 breaths per minute; these breaths deliver a tidal volume remove CO₂, and the other the ventilator "puffs" at 600 breaths per minute.

These puffs hardly deliver any volume, but somehow they keep up pressure and oxygenates the lung and so called High Frequency Jet Ventilation,(HFJV), and the ventilator for obvious reasons is called "Twin Stream". 'TS' stands for twin stream in the following text.

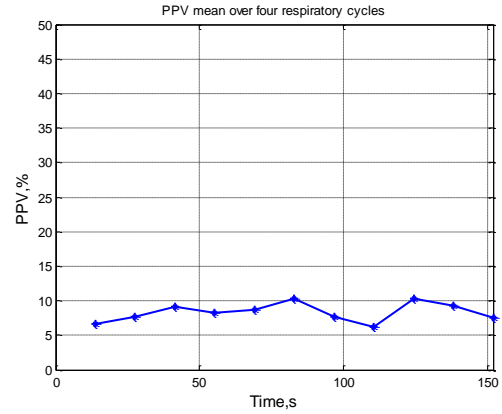
After Recruitment manoeuvre the PEEP level is lowered from 20 to 17, 14, 11, 8 and 5 cm H₂O. At PEEP cm H₂O 5 we changed back to the normal ventilator mode. Afterward second Recruitment manoeuvre is performed in conventional mode of ventilator in which PEEP was reduced to 14 and then 8 cm H₂O. The normal ventilator mode is discriminated from high frequency noise -'TS'- by noting 'SERVO'.

Baseline

Stage 1 : PEEP 5 cm H₂O



(a)

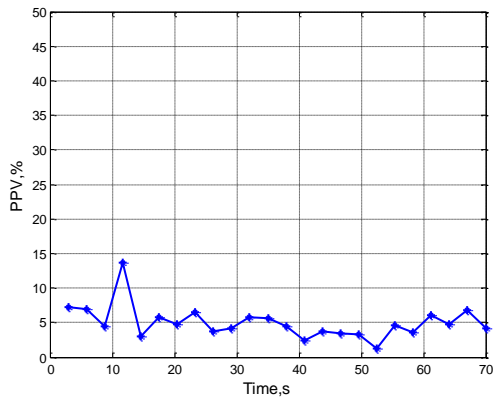


(b)

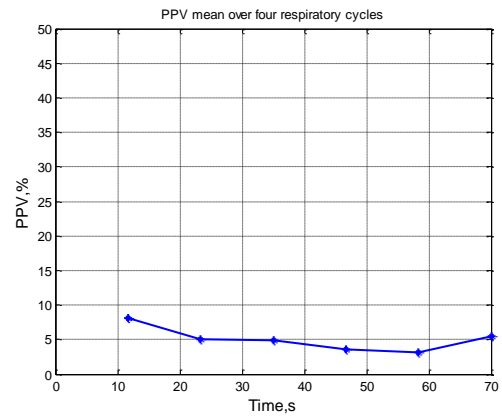
Figure 37 Ventilation in normal ventilator mode at PEEP 5 cm H₂O, considered as the Baseline (BL). PPV and PPV mean over four respiratory cycles are represented in a and b respectively.

After Lavage

Stage 2 : PEEP 5 cm H₂O 'TS'



(a)



(b)

Figure 38 After Lavage –The process of washing lungs with saline-ventilation in normal ventilator mode at BL. PPV and PPV mean over four respiratory cycles are represented in a and b respectively.

After Recruitment Manoeuvre

After Recruitment manoeuvre the PEEP level is depressed from 20 to 17, 14, 11, 8 and 5 cm H₂O and finally. Descending order in PEEP must be abide by PPV sinking and results disclose identical action despite for abnormal PPV value for PEEP = 20 cm H₂O. It must be noted that pulse pressure data was noisy and disturbed by artifacts at higher PEEP levels. At PEEP 5 cm H₂O it returned back to the normal ventilator mode.

Stage 3: PEEP 20 cm H₂O ‘TS’

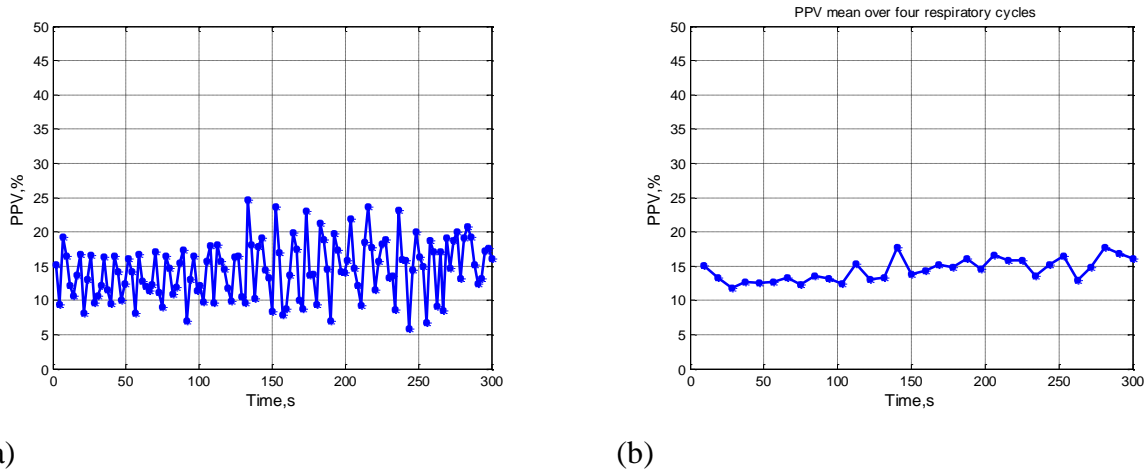


Figure 39 After Recruitment Manoeuvre , ventilation in HFJV mode at PEEP 20 cm H₂O. ‘TS’ stands for Twin Stream. PPV and PPV mean over four respiratory cycles are represented in a and b respectively.

Stage 4: PEEP 17 cm H₂O ‘TS’

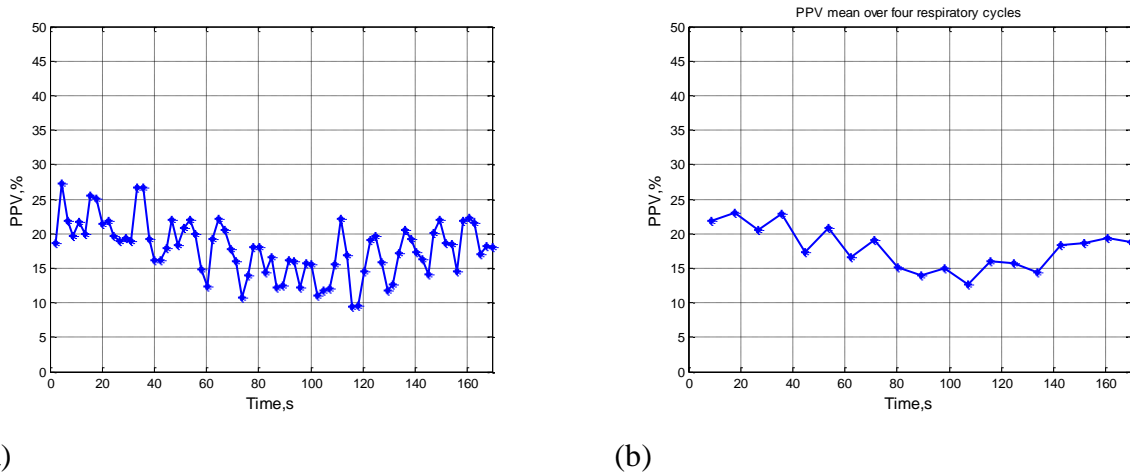
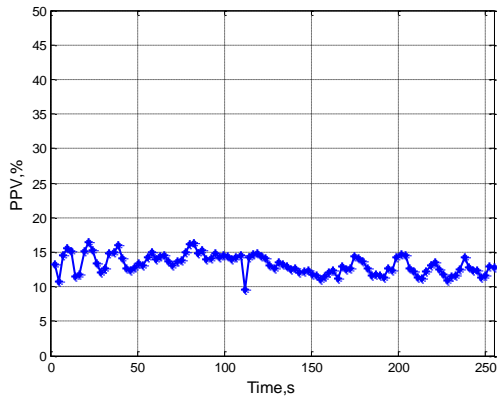
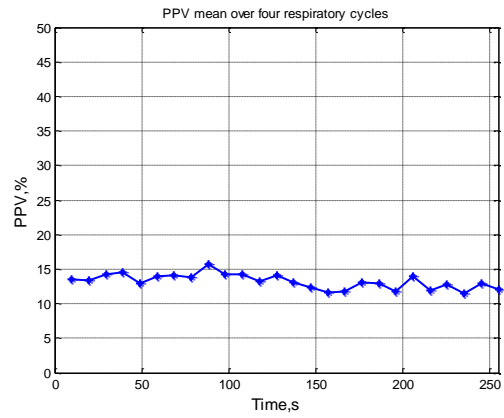


Figure 40 After Recruitment Manoeuvre , ventilation in HFJV mode at PEEP 17 cm H₂O. PPV and PPV mean over four respiratory cycles are represented in a and b respectively.

Stage 5: PEEP 14cm H₂O 'TS'



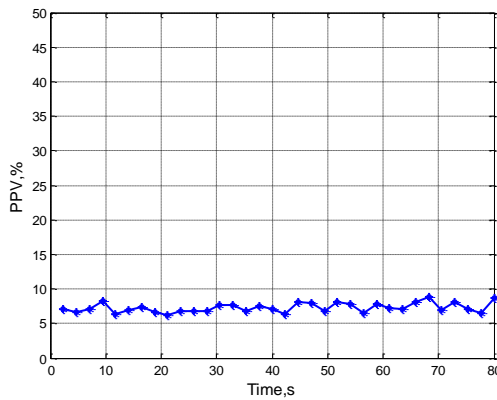
(a)



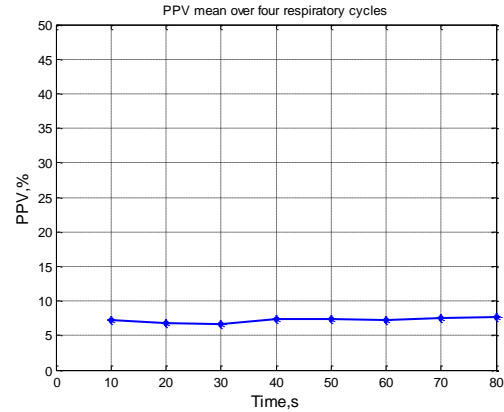
(b)

Figure 41 After Recruitment Manoeuvre , ventilation in HFJV mode at PEEP 14 cm H₂O. PPV and PPV mean over four respiratory cycles are represented in a and b respectively.

Stage 6: PEEP 11cm H₂O 'TS'



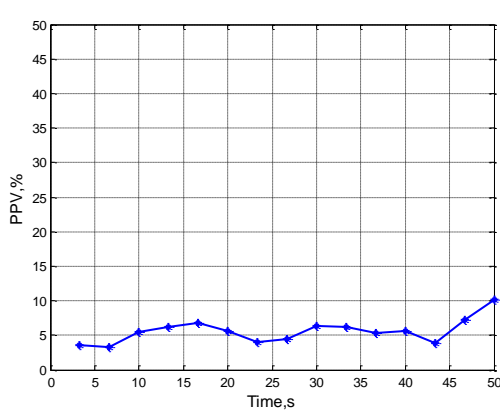
(a)



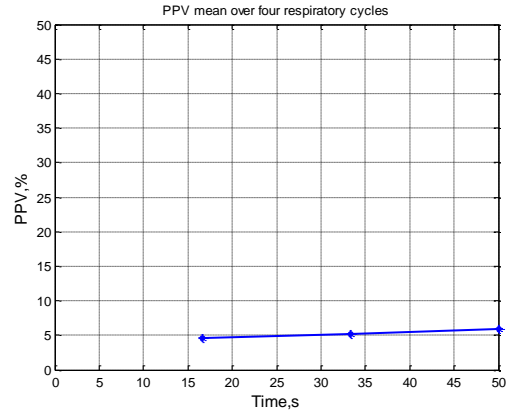
(b)

Figure 42 After Recruitment Manoeuvre, ventilation in HFJV mode at PEEP 14 cm H₂O. PPV and PPV mean over four respiratory cycles are represented in a and b respectively.

Stage 7: PEEP 8 cm H₂O 'TS'



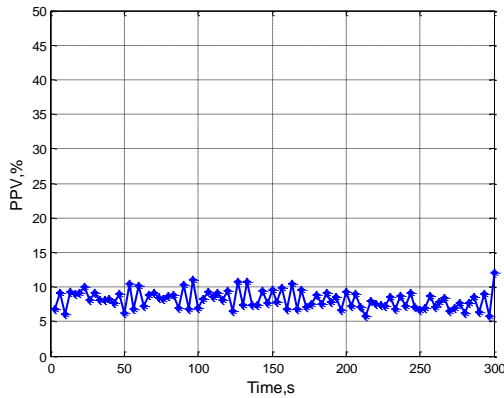
(a)



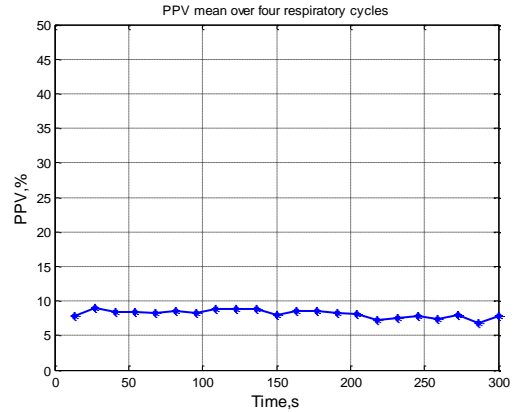
(b)

Figure 43 After Recruitment Manoeuvre, ventilation in HFJV mode at PEEP 8 cm H₂O. PPV and PPV mean over four respiratory cycles are represented in a and b respectively.

Stage 8: PEEP 5 cm H₂O 'TS'



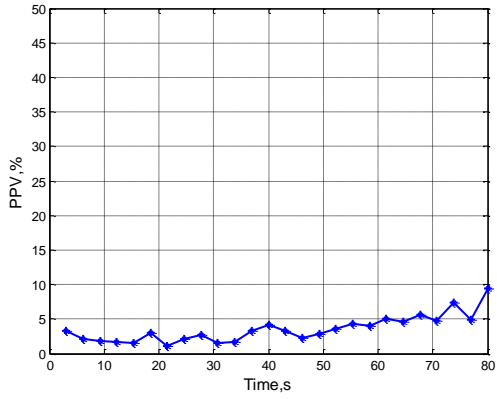
(a)



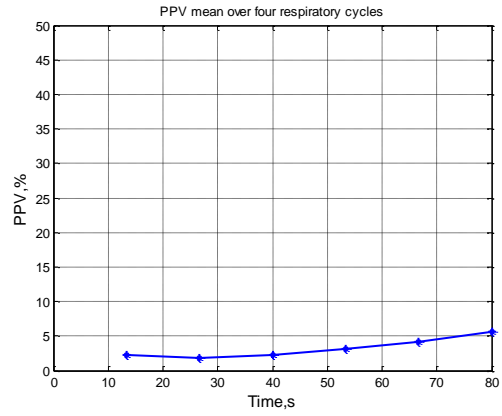
(b)

Figure 44 After Recruitment Manoeuvre, ventilation in HFJV mode at PEEP 5cm H₂O. PPV and PPV mean over four respiratory cycles are represented in a and b respectively.

Stage 9: PEEP 5 cm H₂O Servo



(a)

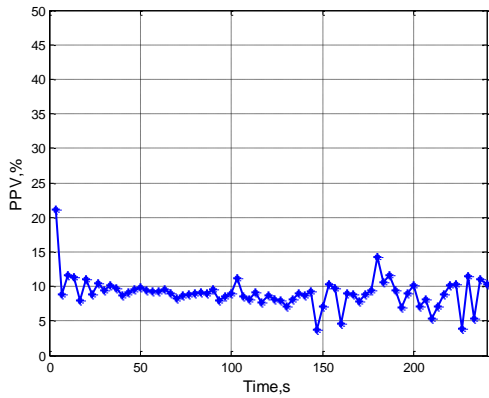


(b)

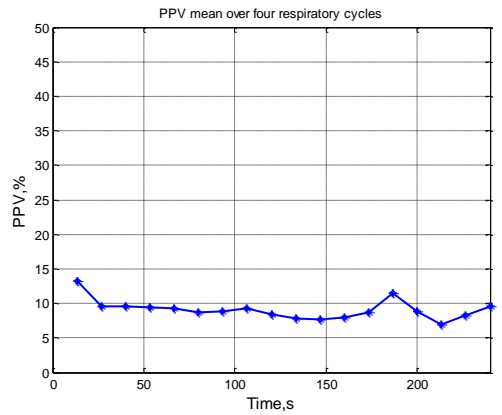
Figure 45 Normal ventilation mode PEEP = 5cm H₂O after first recruitment manoeuvre. PPV and PPV mean over four respiratory cycles are represented in a and b respectively.

After Second RECRUITMENT MANOEUVRE

Stage 10: PEEP 14 cm H₂O Servo



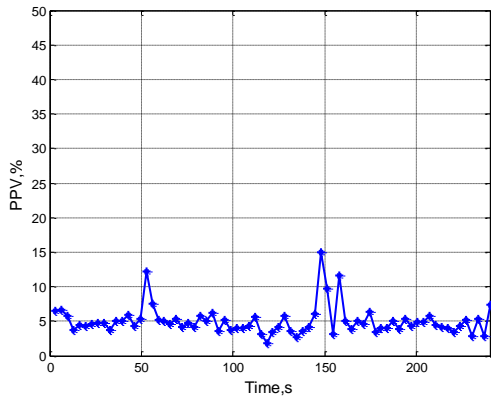
(a)



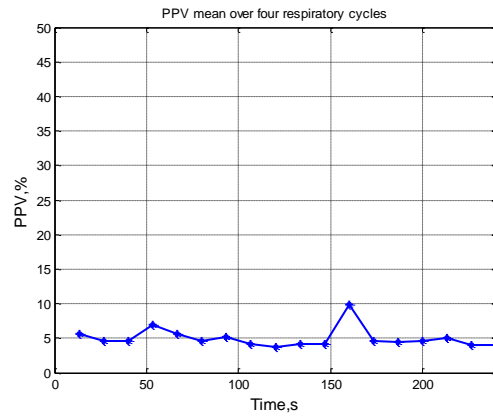
(b)

Figure 46 After second Recruitment Manoeuvre, ventilation in normal mode at PEEP 14 cm H₂O. PPV and PPV mean over four respiratory cycles are represented in a and b respectively.

Stage 11: PEEP 8 cm H₂O Servo



(a)



(b)

Figure 47 After second Recruitment Manoeuvre, ventilation in normal mode at PEEP 11 cm H₂O. PPV and PPV mean over four respiratory cycles are represented in a and b respectively.

The Animal study results arrayed in Table 5 The relationship between PPV and PEEP variation. It was supposed that after first recruitment manoeuvre any drop in PEEP provoke PPV in a decreasing way. The expected behaviour happened in stages 3-8 as in figures 39-44 however in stage 4 a sudden increase for PPV for PEEP 17 cmH₂O was noticed which remains unaccountable.

PEEP Variation	PPV: Mean \pm SD	PPV : Mean \pm SD (Averaged over 4 respiratory cycle)
Stage 1 : PEEP 5 cm H2O (BL)	8 \pm 3	8 \pm 1
Stage 2 : PEEP 5 cm H2O	5 \pm 2	5 \pm 1
Stage 3: PEEP 20 cm H2O TS	14 \pm 7	14 \pm 1
Stage 4 : PEEP 17 cm H2O TS	17 \pm 8	17 \pm 3
Stage 5 : PEEP 14 cm H2O TS	13 \pm 5	13 \pm 1
Stage 6 : PEEP 11 cm H2O TS	7 \pm 3	7 \pm 0.3
Stage 7 : PEEP 8 cm H2O TS	6 \pm 5	6 \pm 0.6
Stage 8 : PEEP 5 cm H2O TS	4 \pm 3	4 \pm 0.5
Stage 9 : PEEP 5 cm H2O	11 \pm 4	11 \pm 1
Stage 10: PEEP 14 cm H2O	9 \pm 5	9 \pm 1
Stage 11: PEEP 8 cm H2O	5 \pm 2	5 \pm 1

Table 5 The relationship between PPV and PEEP variation.

Chapter 5 : Discussion and Conclusion

Signal analysis:

Automatic Beat Detection:

The algorithm's performance in Peak Detection was assessed using ABP dataset publicly available online at <http://bsp.pdx.edu> and results came out to be unaffected by time varying signal morphologies. The algorithm was validated against manual annotation which successfully detected beats of two pressure signals (Abp1,Abp2) with an average sensitivity 99.48 % and positive predictivity 99.91% .

Pulse Pressure Variation Estimation:

The PPV estimation algorithm is Based on M. Aboy algorithms first and second versions [3] [2], while both versions provide the possibility of estimating PPV utterly independent from measuring airway pressure waveform. The respiratory frequency can be estimated from the pulse pressure signal. The first algorithm introduced in 2004 was for mechanically ventilated patients based on automatic beat detection algorithm, kernel smoothing, and rank order filtering. The second version presented in 2009 specifically address abrupt hemodynamic changes and claim for measuring PPV not only during normal hemodynamic status but also as a useful predictor of fluid responsiveness during periods of severe blood loss.

The algorithm performance was compared against a commercial functional hemodynamic monitoring system LiDCO plus (LiDCO Ltd, Cambridge ,United Kingdom) results and agreement between calculated PPVs (mean + SD) was 0.58 ± 1.31 .

Results:

The algorithm performed satisfactorily although results may not have been as hypothesized. This may probably be described the scarcity of patients (two) and the noisy physiological environment with many factors concurrently affecting measurements, but with a trend that may be explained by the physiological model.

Limitations:

PPV calculation can only be performed during mechanical ventilation during anaesthesia. The patient must be in sinus rhythm - the normal beating of the heart -as arrhythmia per se (see

paragraph on heart cycles) imply variable length of filling phase and thus varying SV. The essential tidal volume demonstrating PPV most efficiently has been known to be approximately 8 mL/kg. This need in is not in accordance with the required tidal volume to remove CO₂ and oxygenate the patient. As the respiratory induced variations in venous return have to be transmitted through the pulmonary circulation, this pulmonary vascular bed should not be of high vascular resistance and finally it has been noticed that the heart should be without valvular disease (insufficiency causing regurgitation during late systole, or stenosis dampening the transmission of the respiratory induced variations).

The experimental setup:

The measurements were usually strictly controlled as Baseline-measurement and Intervention-measurement; however the measurements were performed during clinical situations where many interventions and factors beyond the control may affect cardiac function and venous return. The measurements and results thus rather demonstrate the difficulty of obtaining stable, undisturbed conditions for the assessment of the effect of the interventions (tidal volume, fluid volume, vasopressor) and while the algorithm as such performed satisfactorily, the clinical situation does not always allow for a clear-cut use and result.

In the study different kinds of excitation of the system was tried: Minute Volume, Fluids, Vasopressors, yet Inotropes are not tested as they were not indicated by the clinical situation.

I have analysed the algorithm in two patients with deliberate manipulation of volume (fluid resuscitation), changes in intrathoracic pressure by varying minute volume ventilation (affecting Pms-RAP) and changes in vasomotor tone. No attempts were made at changing heart efficiency by the use of Inotropes or Betablockers. The algorithm was tested during surgical operation where it is difficult to obtain stable conditions when performing singular interventions (“noisy” physiological environment).

Future works:

The algorithm performed satisfactorily although the results may not have been as hypothesized. This may probably be ascribed the scarcity of patients (two) and the noisy physiological environment with many factors concurrently affecting measurements. From this it is freely

available, and possible to conclude that the use of PPV may add important clinical important information for decision making in the operative setting.

References

1. **Michard, Frédéric M.D., Ph.D.** *Changes in arterial pressure during mechanical ventilation.* Anesthesiology, Volume: 103, page(s) 419-428, August 2005.
2. **Mateo Aboy, Cristina Crespo, and Daniel Austin** *An Enhanced Automatic Algorithm for Estimation of Respiratory Variations in Arterial Pulse Pressure During Regions of Abrupt Hemodynamic Changes.* IEEE Transactions On Biomedical Engineering, Volume. 56, Page(s) : 2537 - 2545 October 2009.
3. **Mateo Aboy, James McNames, Tran Thong, Charles R. Phillips** *A Novel Algorithm to Estimate the Pulse Pressure.* IEEE Transactions on Biomedical Engineering, Vol.51, pages: 2198 - 2203 2004. Dec. 2004.
4. **Guyton, A.C. & Hall, J.E.** *Textbook of Medical Physiology*. 11th edition. Philadelphia : Elsevier Saunder, 2006.
5. <http://www.cvphysiology.com/Heart%20Disease/HD002.htm>.
6. <http://www.cvphysiology.com/Cardiac%20Function/cardiac%20cycle%20fig.htm>.
7. **Frédéric Michard, Marcel R Lopes and Jose-Otavio C Auler Jr.** *Pulse pressure variation: beyond the fluid management of patients with shock.* Critical Care, May 2007.
8. **Ornstein E, Eidelman LA, Drenger B, Elami A, Pizov R.** *Systolic pressure variation predicts the response to acute blood loss.* Volume 10, Page(s) 137-140, March 1998.
9. **W.W. Nichols and M. F. O'Rourke.** *McDonald's Blood Flow in Arteries: Theoretical, Experimental and Clinical Principles*, 5th Edition, April 2005.
10. **W. Holsinger, K. Kempner, and M. Miller.** *A QRS preprocessor based on digital differentiation,* IEEE Transactions on Biomedical Engineering, Volume: BME-18, May 1971, page(s): 212 - 217.
11. **V. Afonso, W. Tompkins, T. Nguyen, and S. Luo.** *ECG beat detection using filterbanks,* IEEE Transactions on Biomedical Engineering, Volume: 46, Feb. 1999, page(s): 192 - 202 .
12. **S. Kadambe, R. Murray, and G. Boudreaux-Bartels.** *Wavelet transform based QRS complex detector.* IEEE Transactions on Biomedical Engineering, Volume: 46, page(s): 838 - 848, July 1999
13. **Michard F, Boussat S, Chemla D, Anguel N, Mercat A, Lecarpentier Y, Richard C, Pinsky MR, Teboul JL.** *Relation between respiratory changes in arterial pulse pressure and*

fluid responsiveness in septic patients with acute circulatory failure. Critical Care Medicine, Volume 162, page(s):134-138, July 2000.

14. <http://www.oucom.ohiou.edu/cvphysiology/CF008.htm>.

15. **Mateo Aboy***, **James McNames**, **Daniel Tsunami**, **Miles S. Ellenby**, and **Brahm Goldstein**, *An Automatic Beat Detection Algorithm for Pressure Signals.* IEEE Transactions on Biomedical Engineering , Volume: 52, page(s): 1662 - 1670, Oct. 2005.

16. **Hayes, M. H.** *Statistical Digital Signal Processing and Modeling*, New York : John Wiley & Sons, 1996.

17. **Cannesson M**, **Aboy M**, **Hofer C**, **Rehman M.** Pulse Pressure Variation: Where Are We Today?, Journal of Clinical Monitoring and Computing, 2010.